

Fig. 11 Interannual East Asian summer monsoon JJA 850hPa wind anomalies and precipitation anomalies based on linear regression with the revised JJA Wang-Fan 850hPa zonal wind index for **a** JRA25/GPCP, **b** CMIP5 MMM, **c** CMIP3 MMM, **d** gfdl cm2.0 model, **e** fgoals1.0-g, **f** HadGEM2-ES, and **g** INM-CM4. **d** and **e** are the models with the largest and smallest 850hPa wind pattern correlations compared to JRA25 850hPa wind anomalies, and **f** and **g** are the models with the largest and smallest precipitation pattern correlations compared to GPCP. Also given in **a** is the pattern correlation of JRA25 with NCEP/NCAR Reanalysis and GPCP with CMAP, respectively, and in **b-g** are the model pattern correlations with JRA25 and GPCP over the region 100°E-140°W, 0°-50°N. The units for the 850hPa wind anomalies are ms^{-1} and for precipitation anomalies the units are mm day^{-1} . The JRA25 reanalysis, the NCEP-NCAR reanalyses, the GPCP, and CMAP data are for 1979-2007. The model data is for 1961-1999

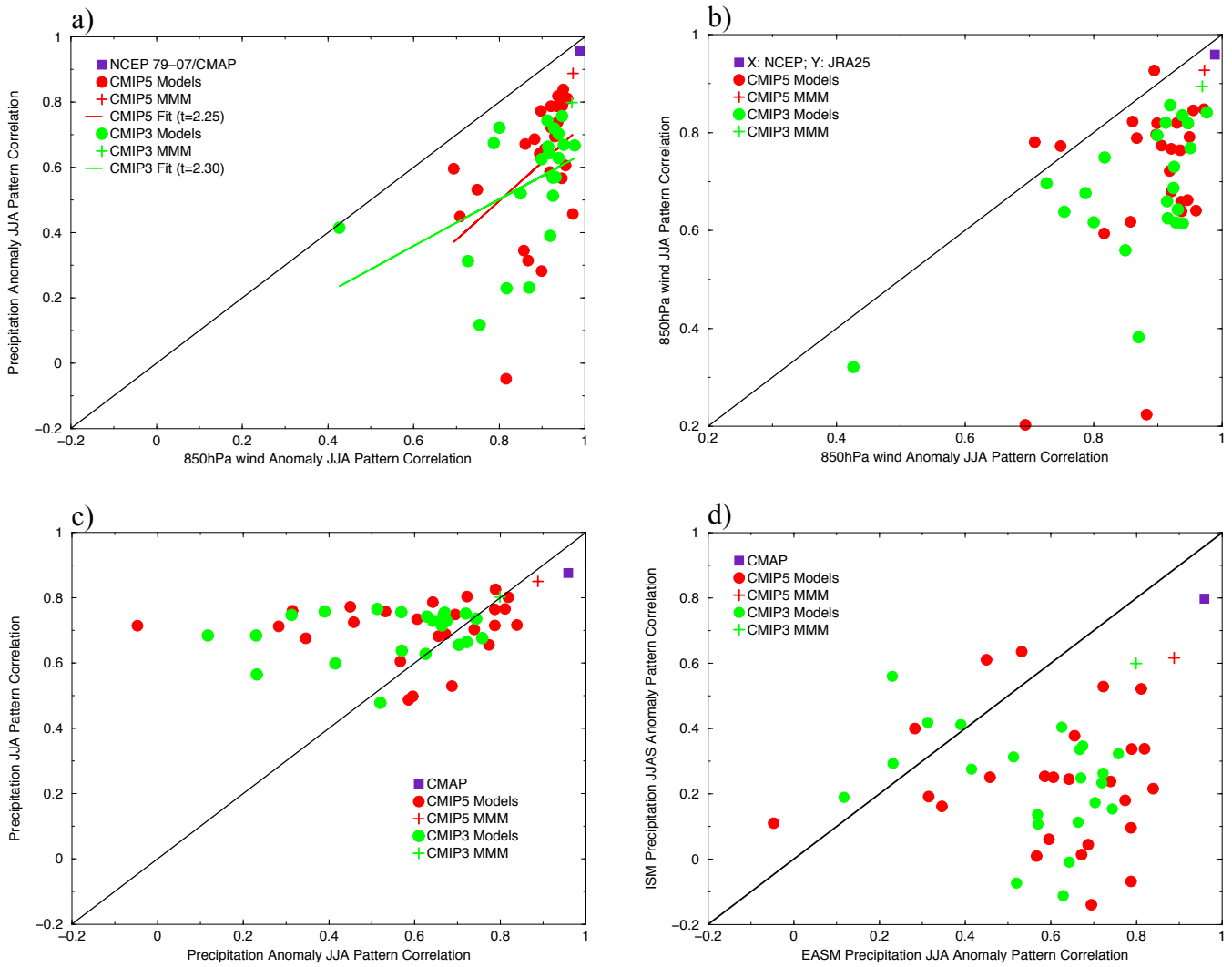
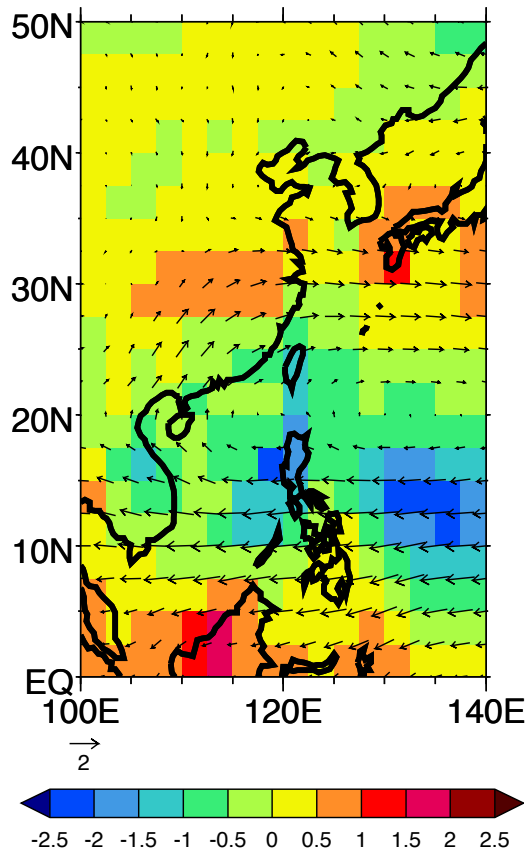
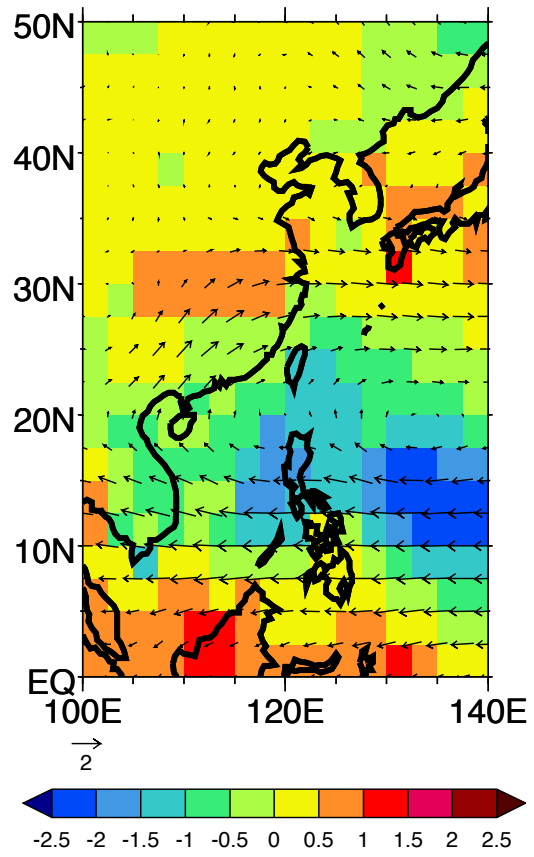


Fig. 12 **a** Scatterplot of the pattern correlation with observations of simulated JJA 850hPa wind anomalies vs. the pattern correlation with observations of simulated JJA precipitation anomalies over East Asia. The skill is relative to JRA25 and GPCP over the region 100°E-140°E, 0°-50°N. **b** Scatterplot of the pattern correlation with observations of simulated JJA 850hPa wind anomalies vs. the pattern correlation with observations of the simulated JJA 850hPa wind climatology. The skill is with respect to JRA25 on the x-axis, and with respect to ERA40 on the y-axis. **c** Scatterplot of the pattern correlation with GPCP of simulated JJA precipitation anomalies vs. the pattern correlation with observations of the simulated JJA precipitation climatology. **d** Scatterplot of the pattern correlation with GPCP of simulated JJA precipitation anomalies over the East Asia (as in Figs. 12a and 12c) vs. the pattern correlation with GPCP of simulated JJAS precipitation anomalies over the Indian Summer Monsoon (as in Fig. 9b)

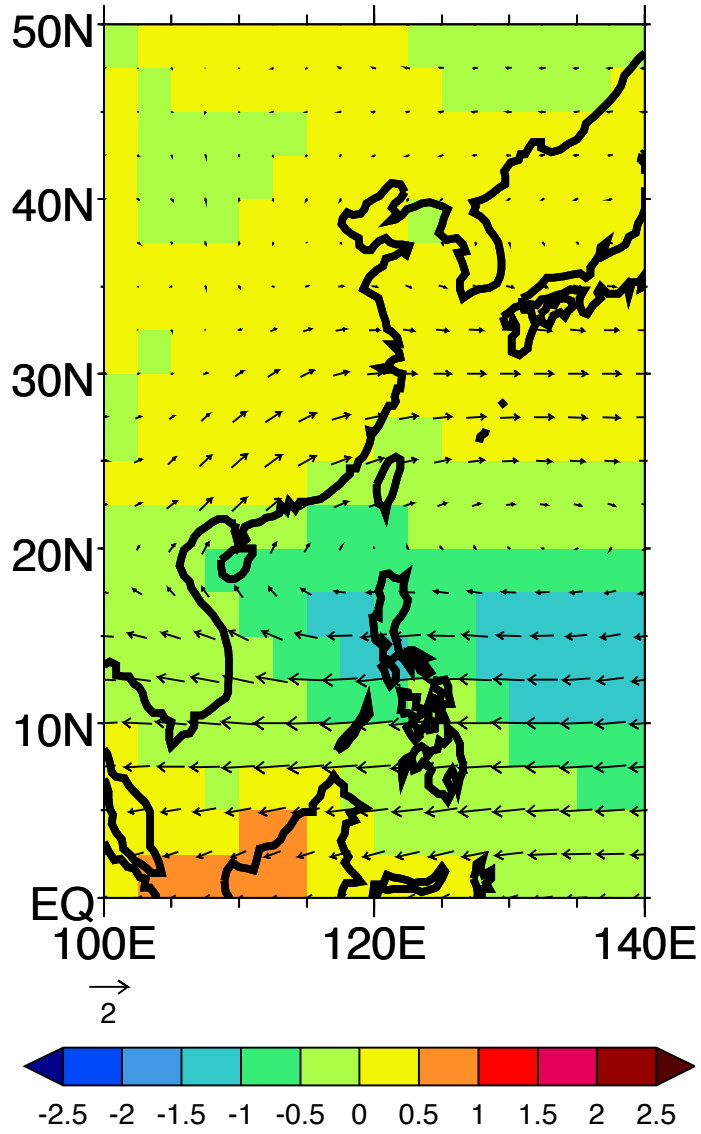
JRA25/GPCP (1979-2007)



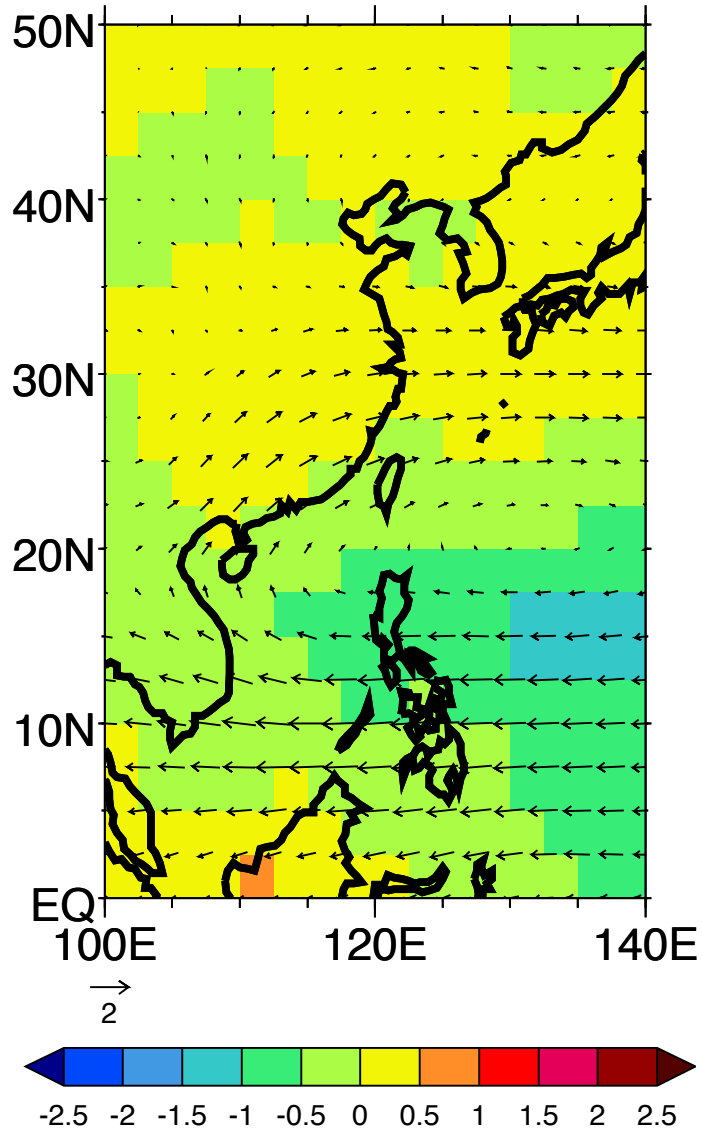
CMAP/NCEP (1979-2007)



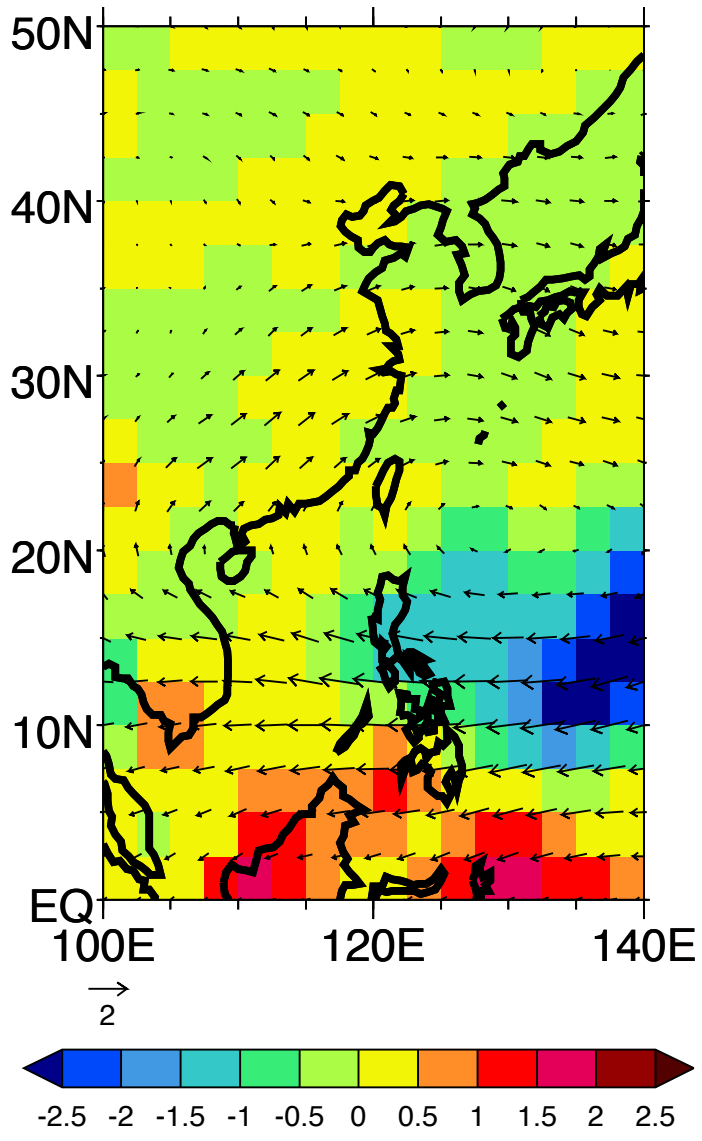
CMIP5 MMM



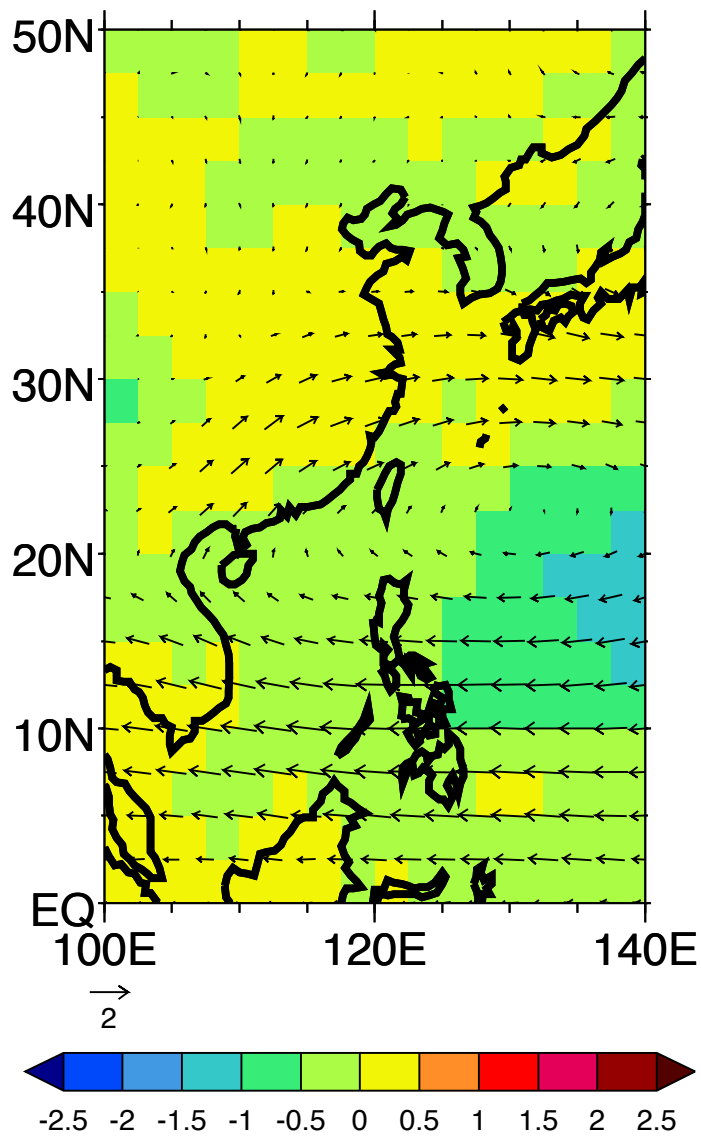
CMIP3 MMM



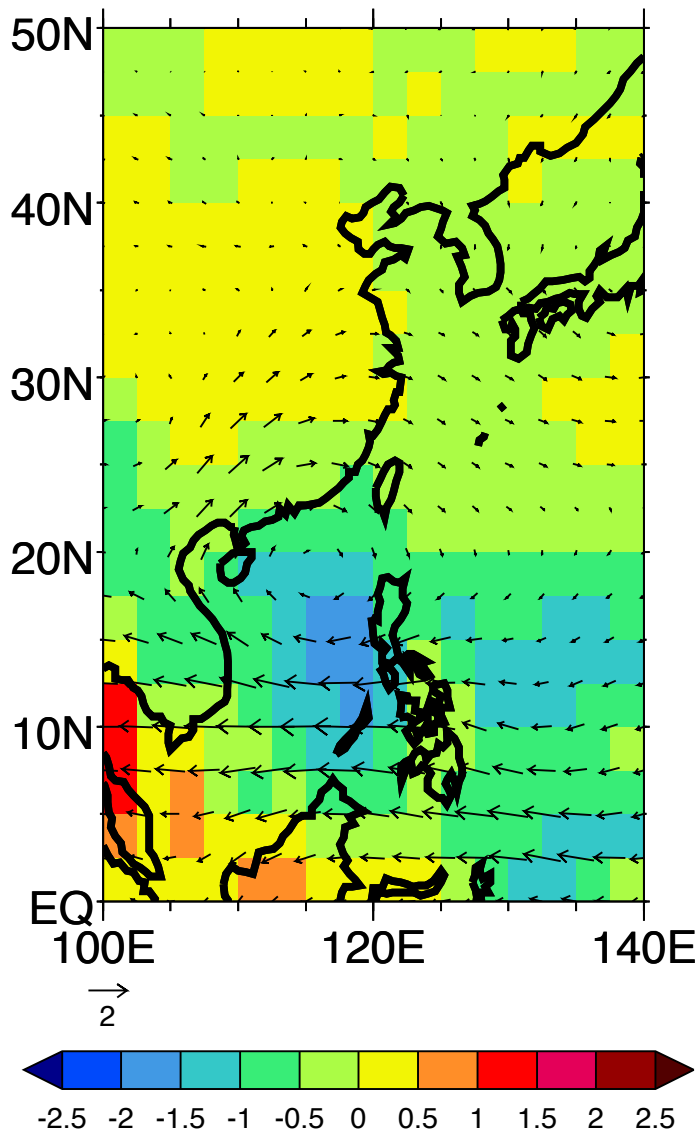
BCC-CSM-1



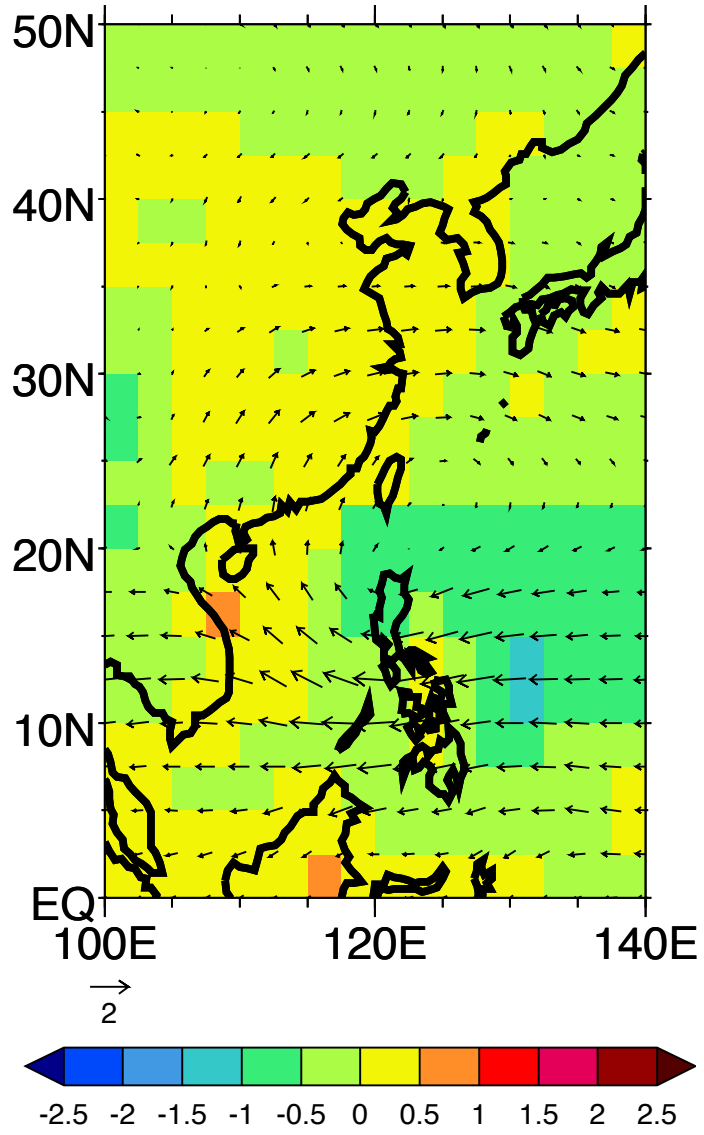
bccr-bcm2.0



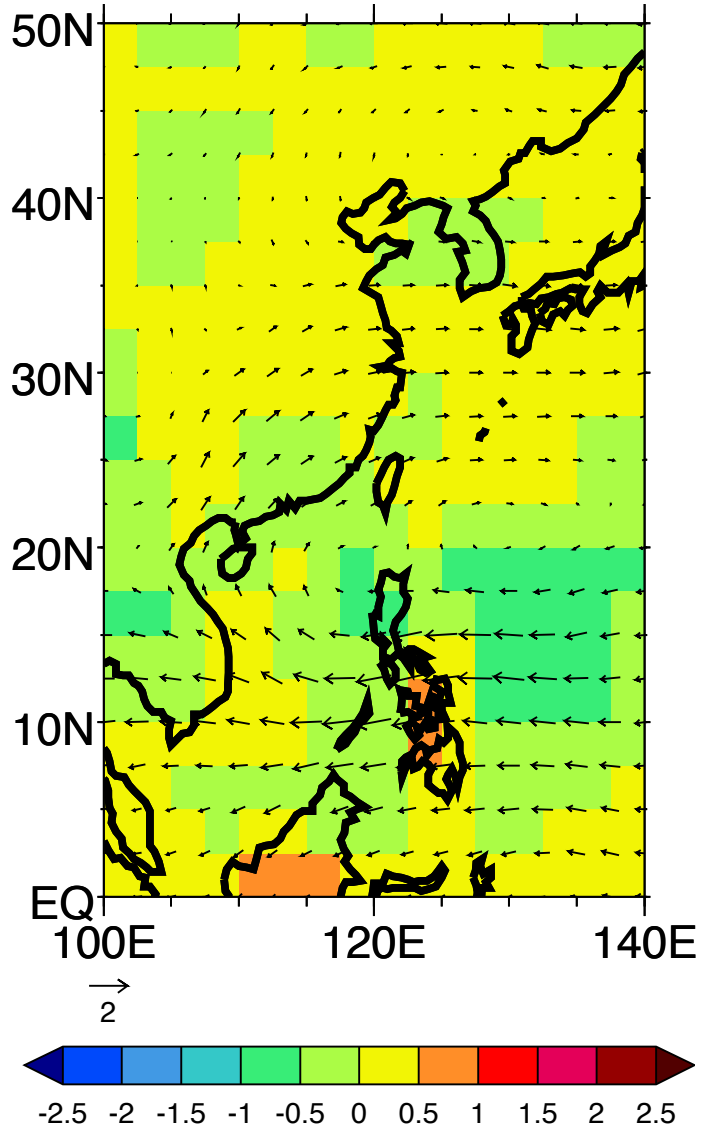
CanESM2



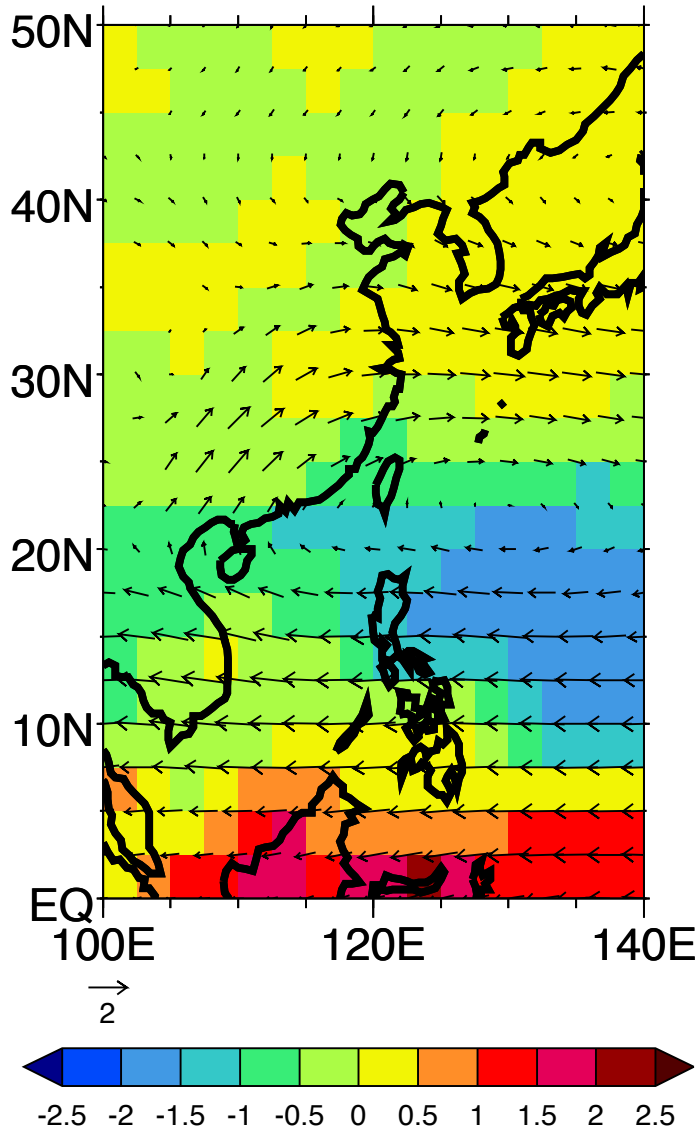
cgcm3.1 (t47)



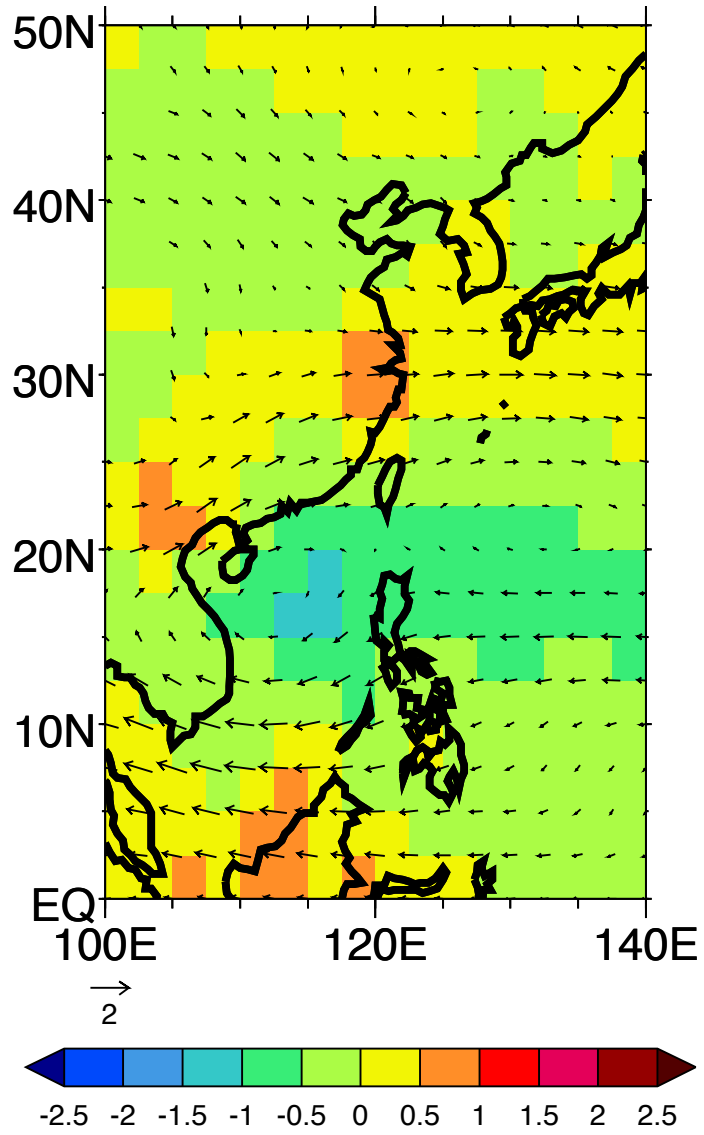
cgcm3.1 (t63)



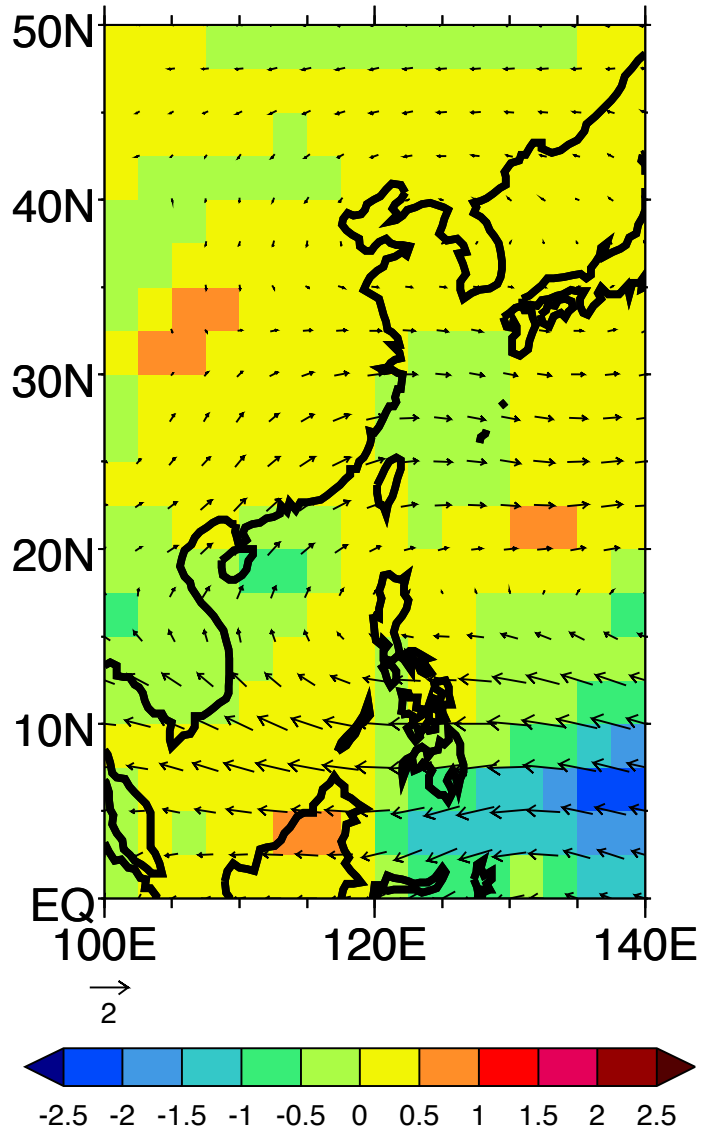
CCSM4



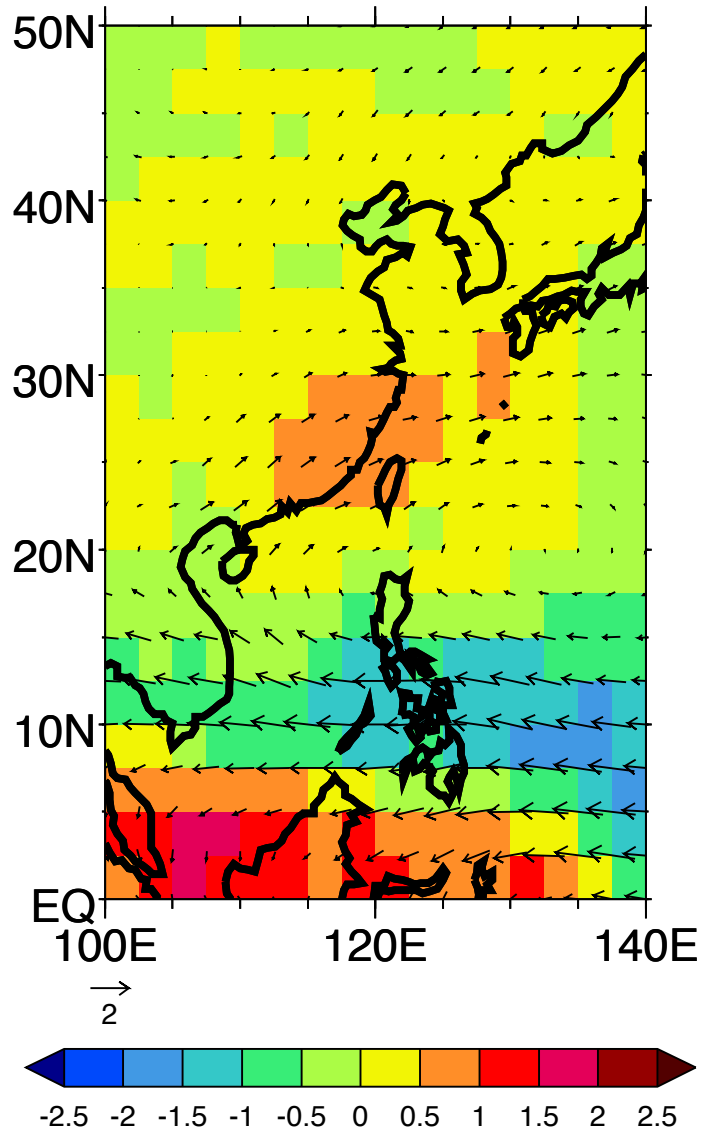
ccsm3



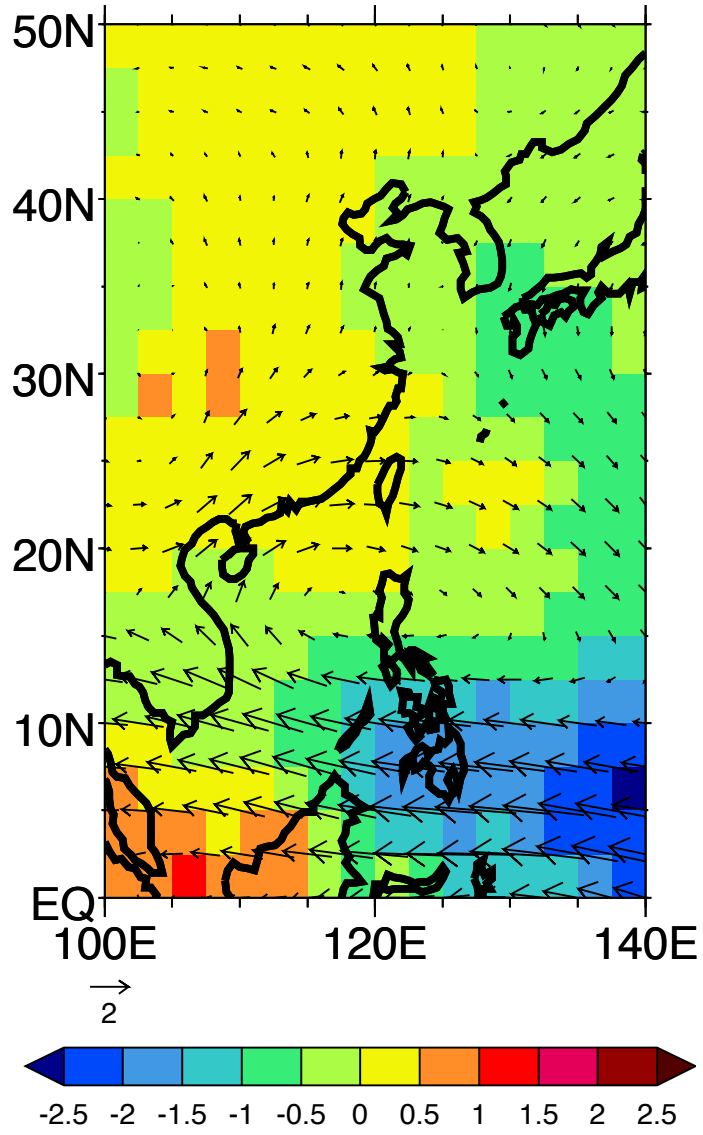
pcml



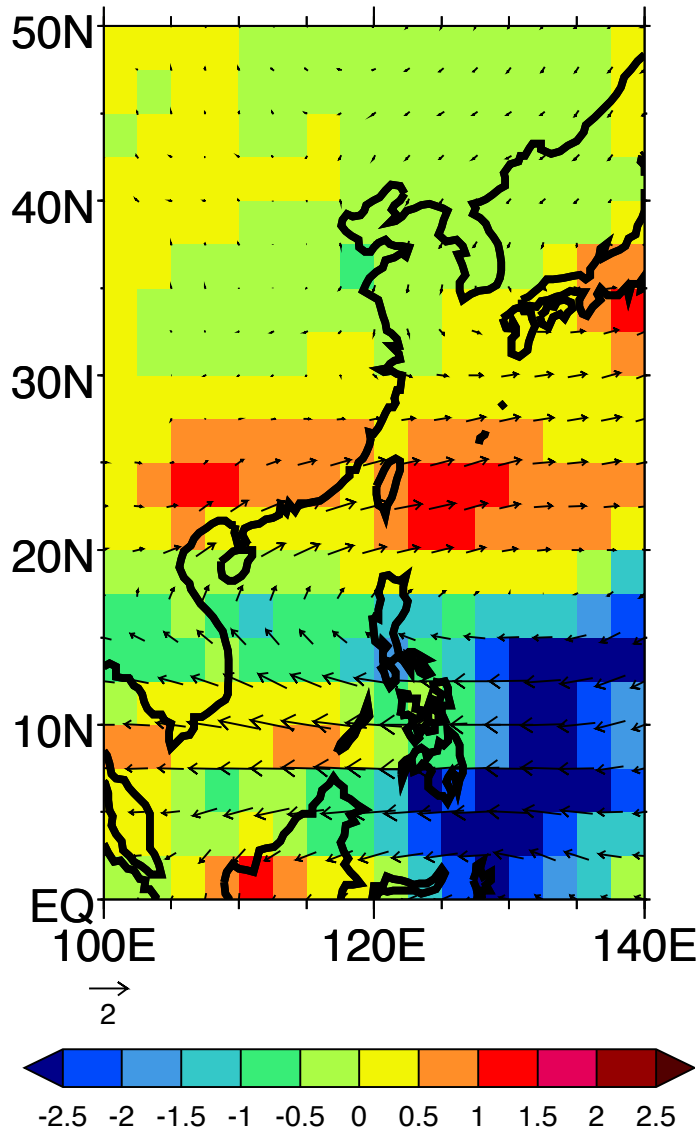
CNRM-CM5



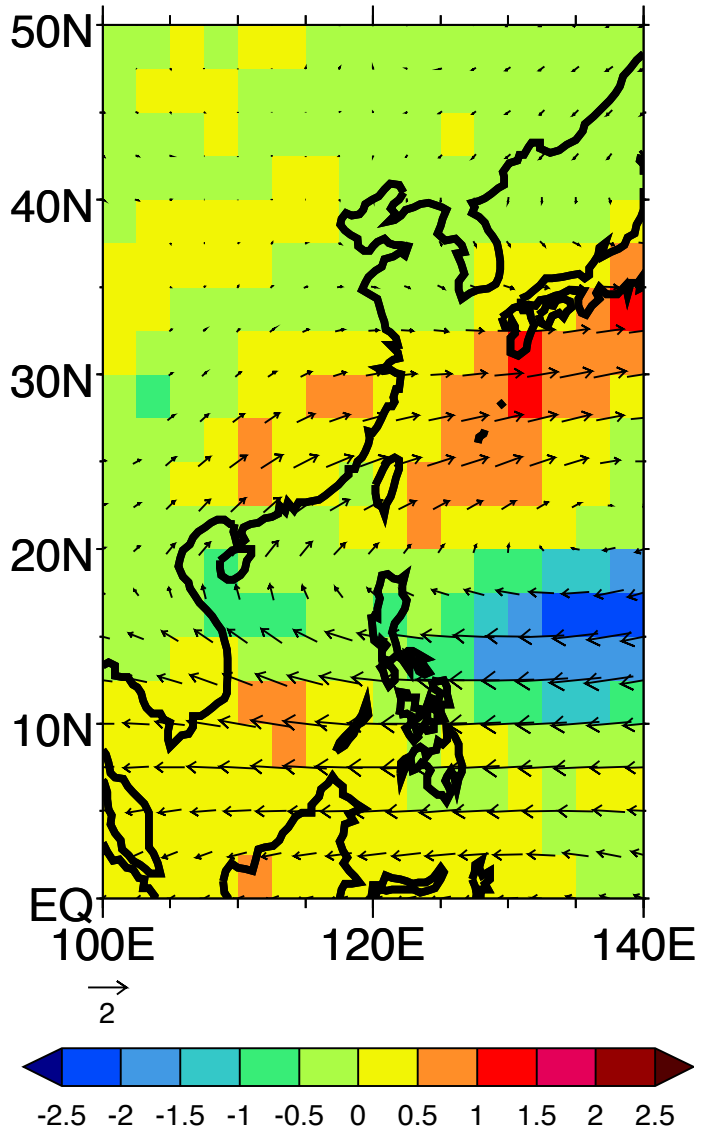
cnrm-cm3



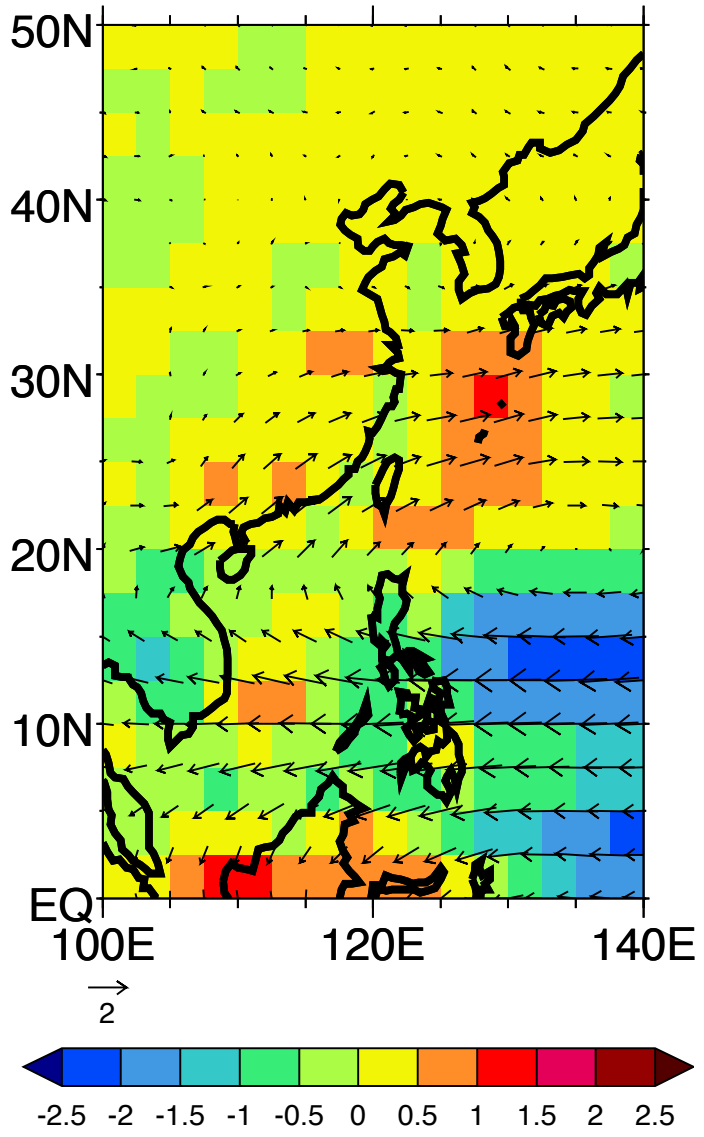
CSIRO-Mk3.6.0



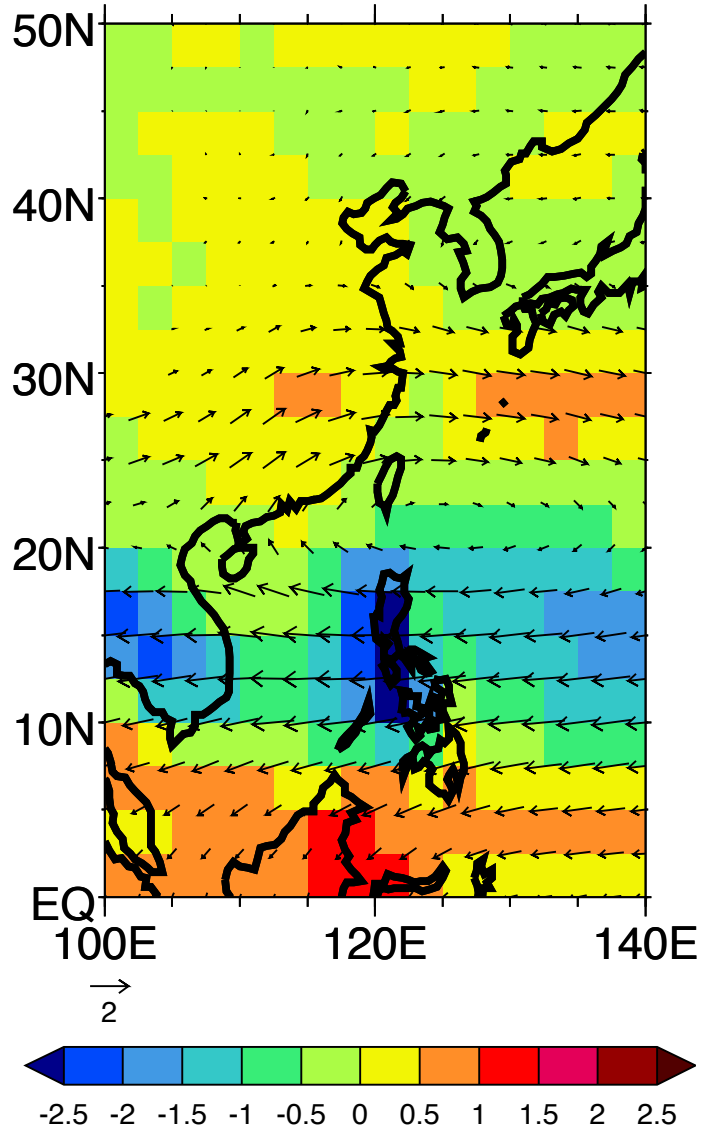
csiro-mk3.0



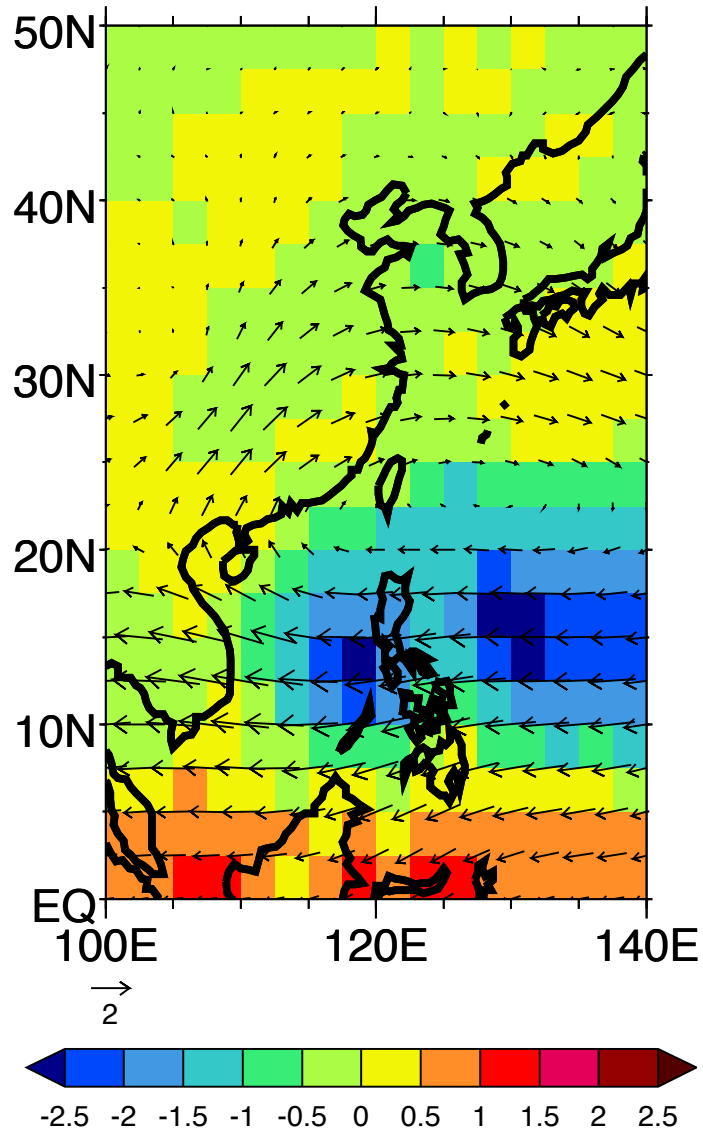
csiro-mk3.5



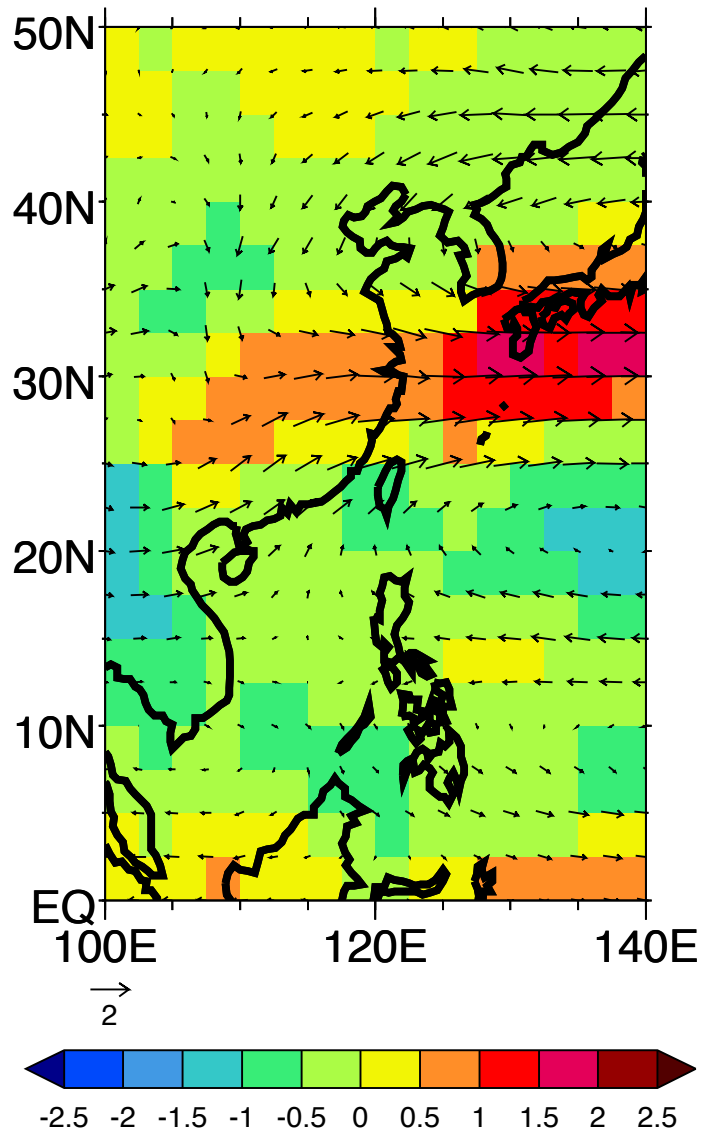
FGOALS-g2



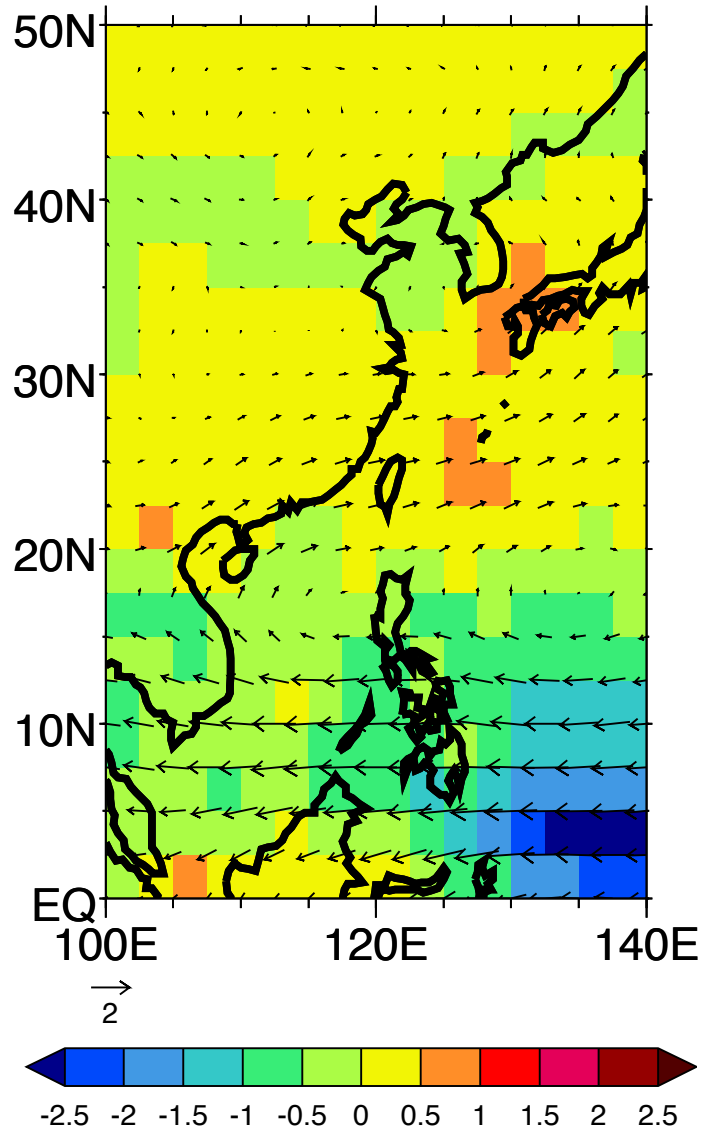
FGOALS-s2



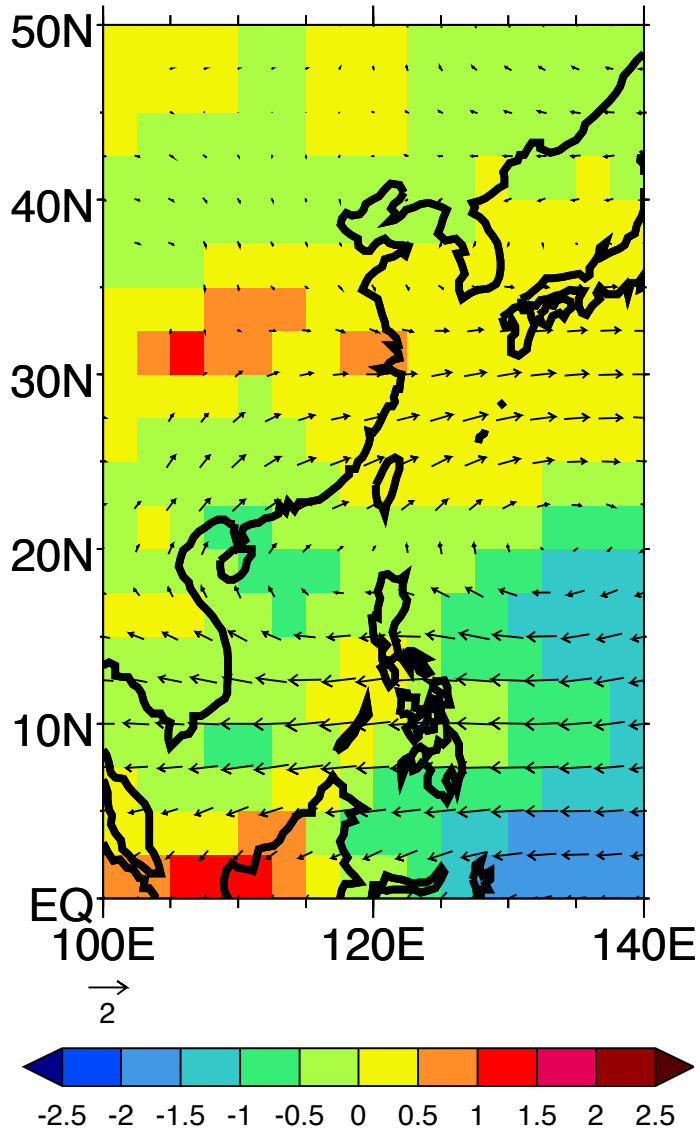
fgoals-g1.0



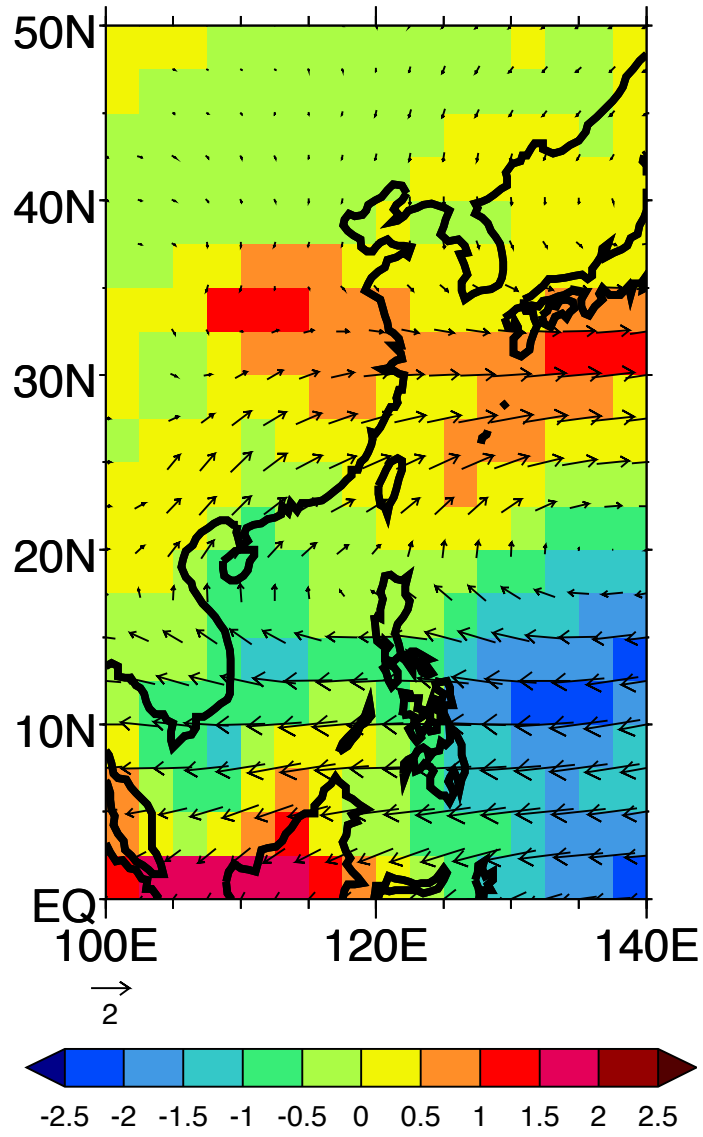
GFDL-CM3



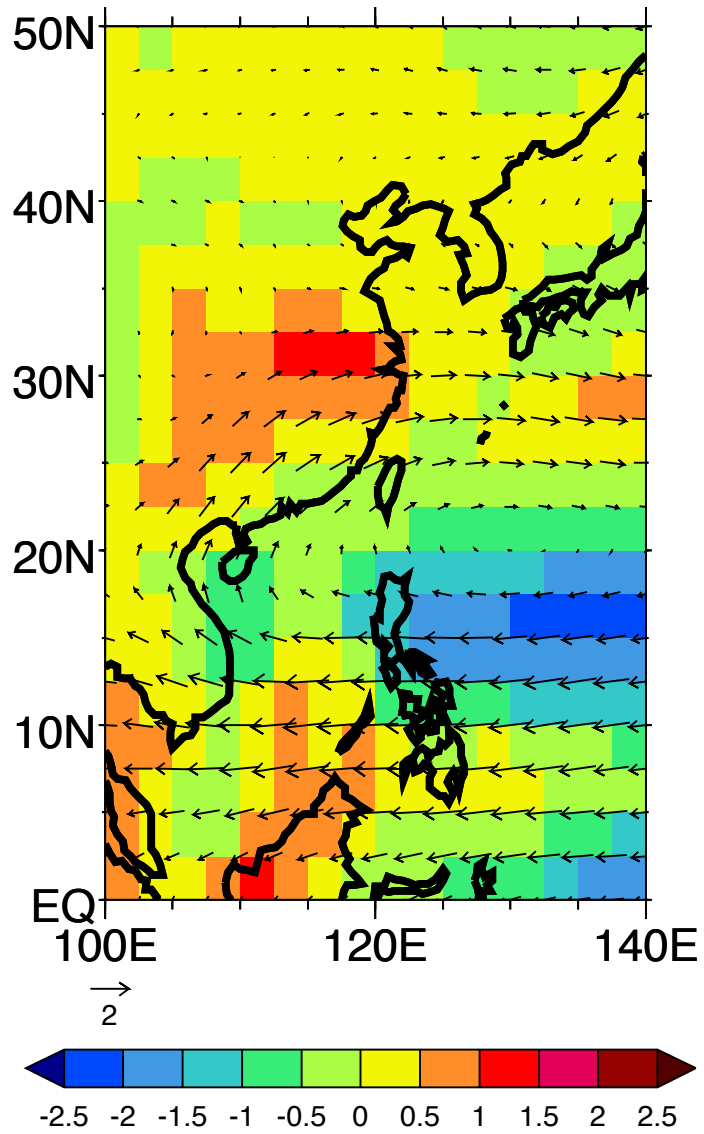
GFDL-ESM2G



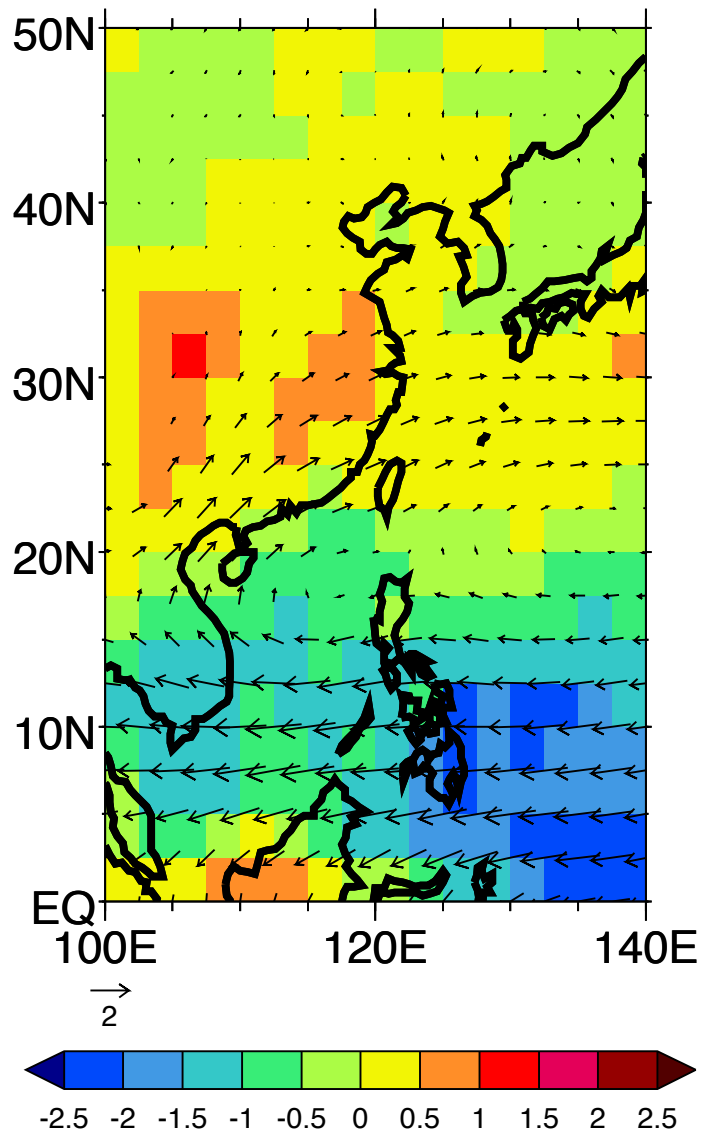
GFDL-ESM2M



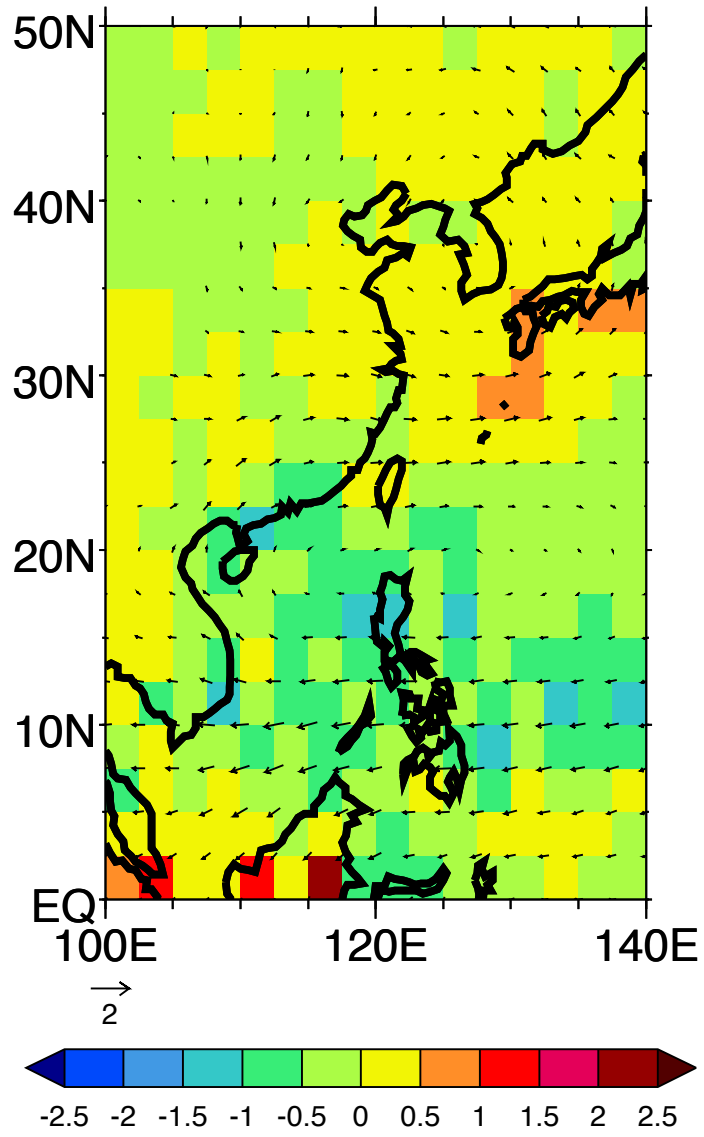
gfdl-cm2.0



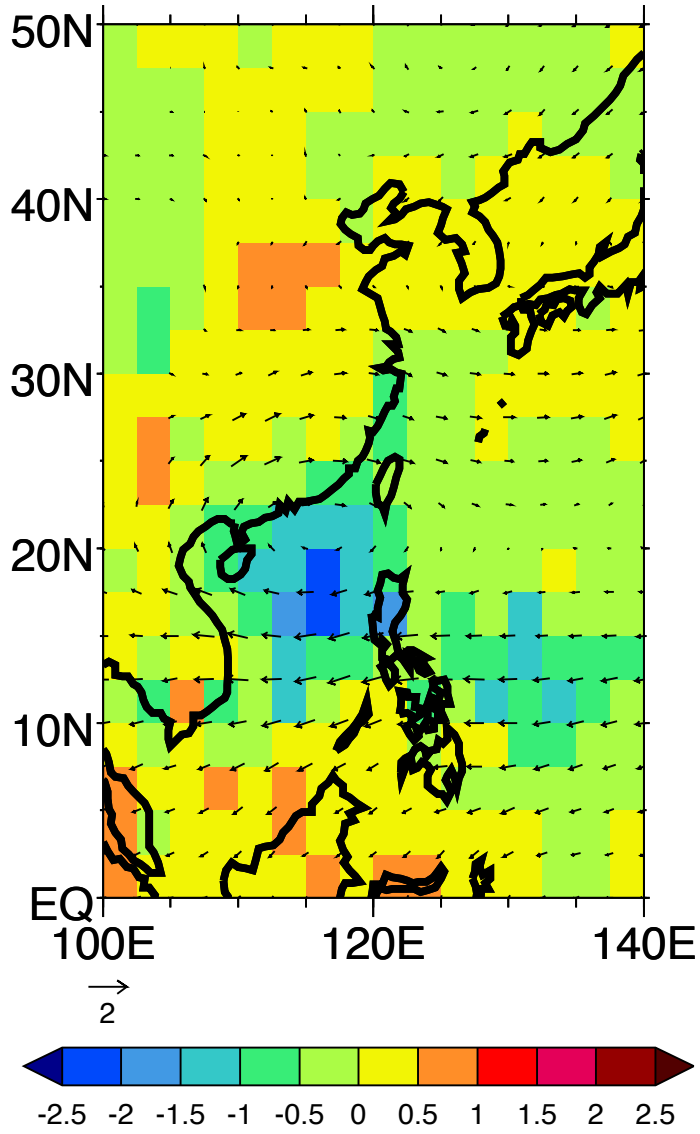
gfdl-cm2.1



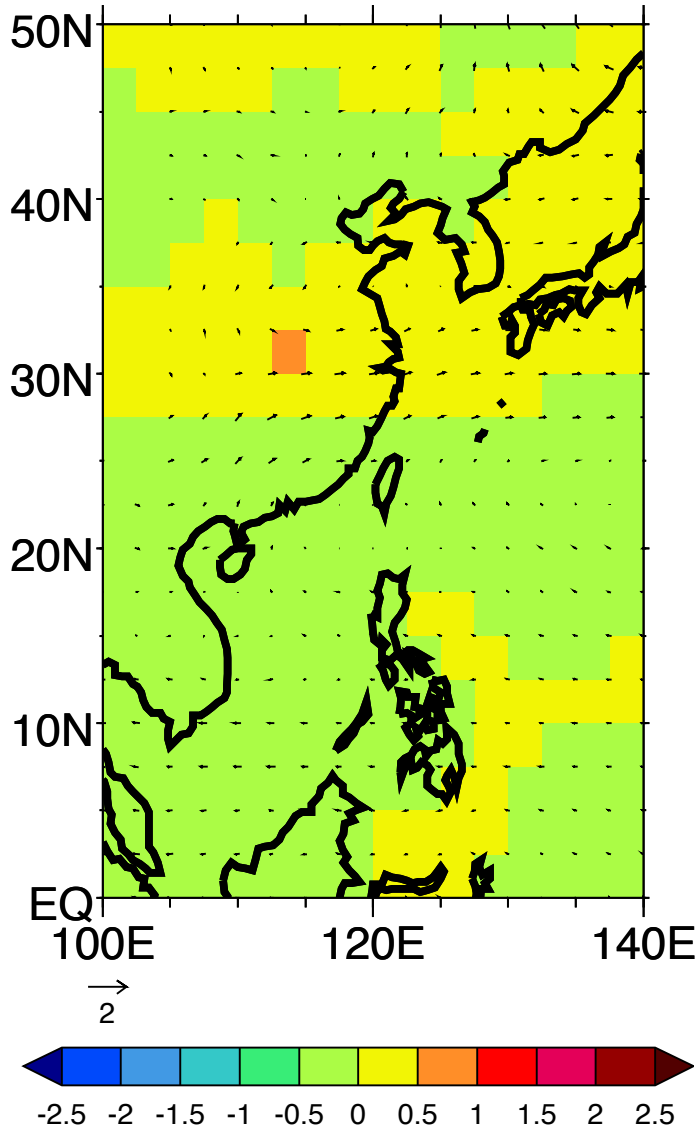
GISS-E2-H



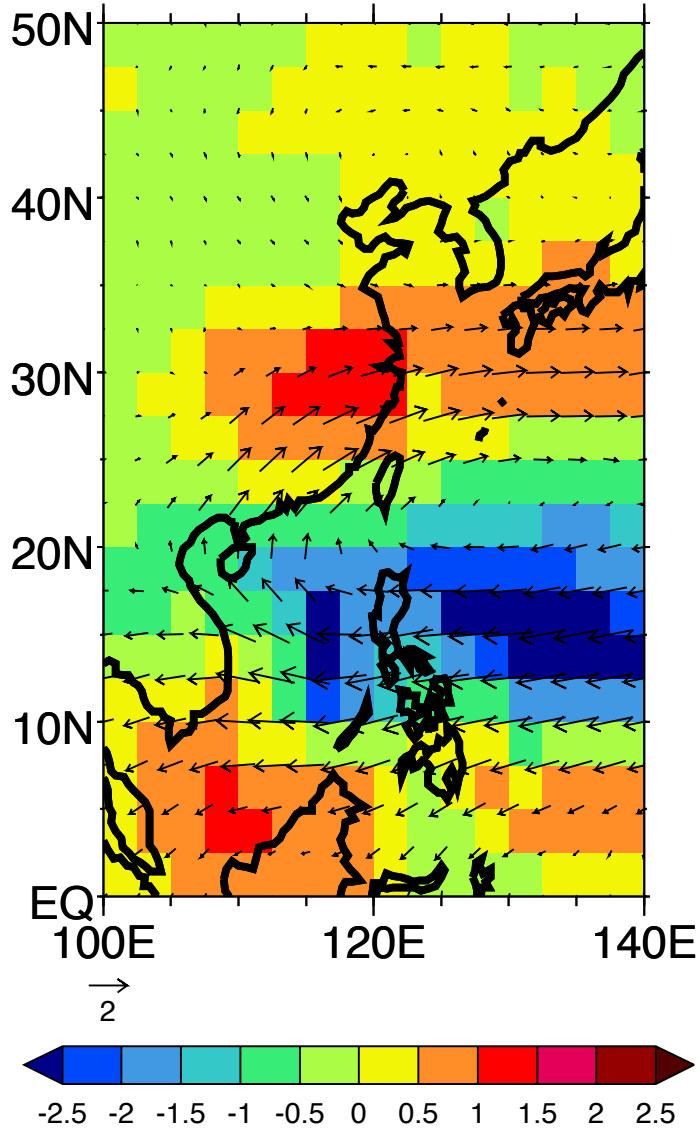
GISS-E2-R



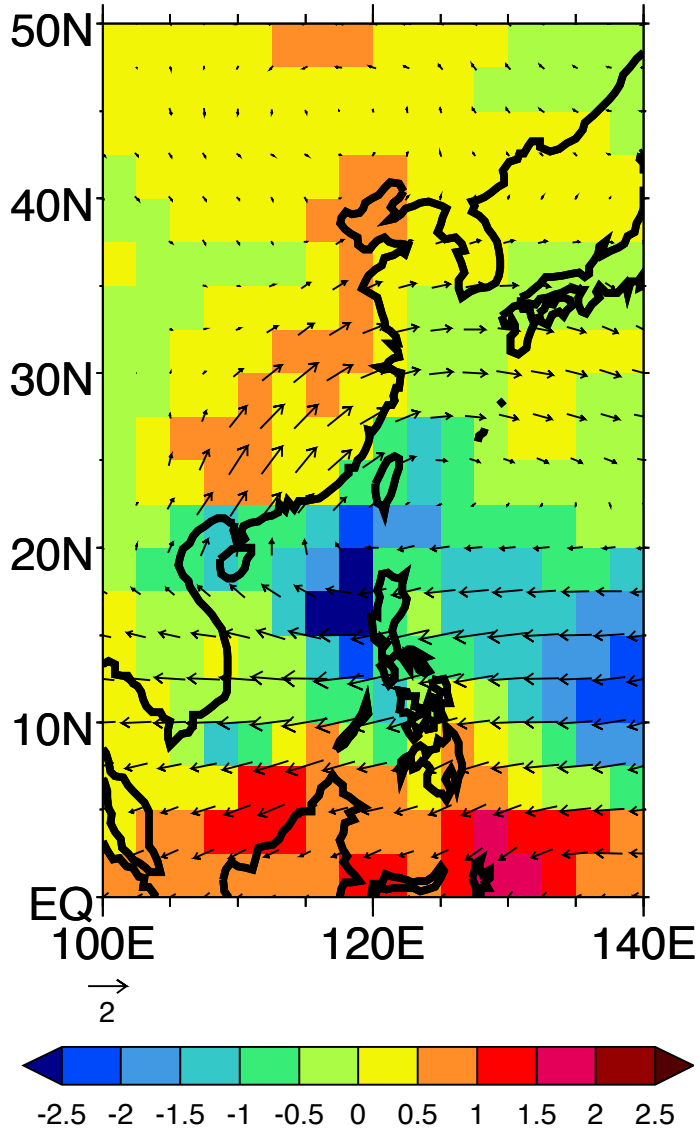
giss-aom



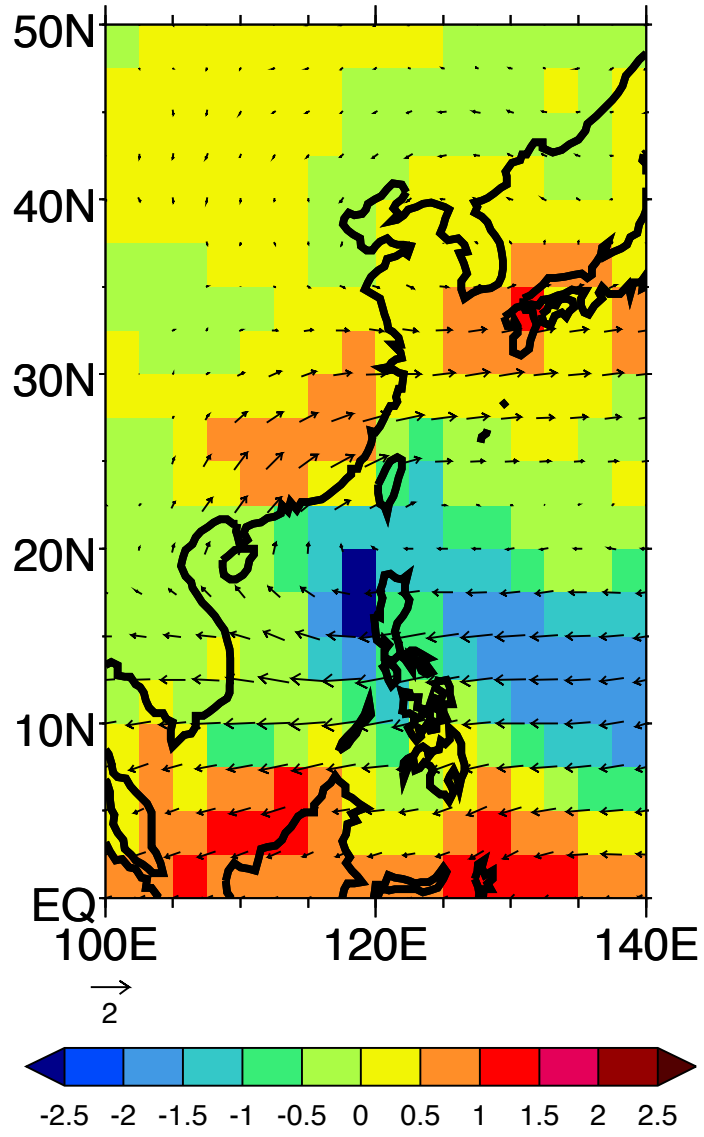
HadCM3



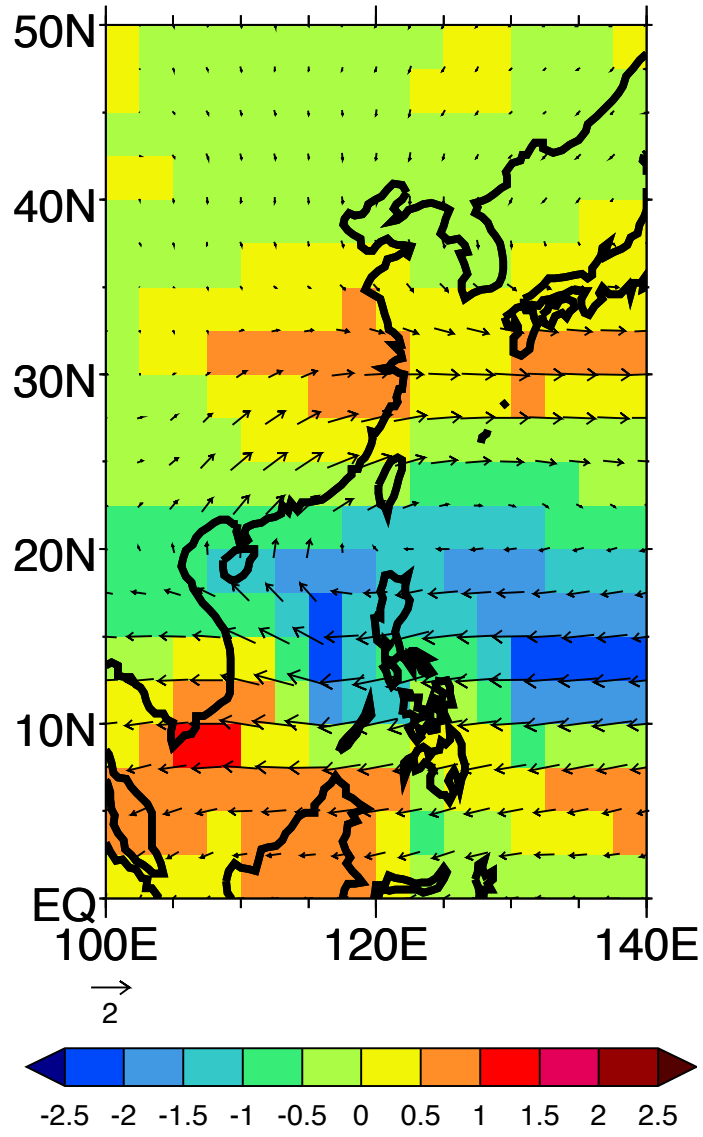
HadGEM2-CC



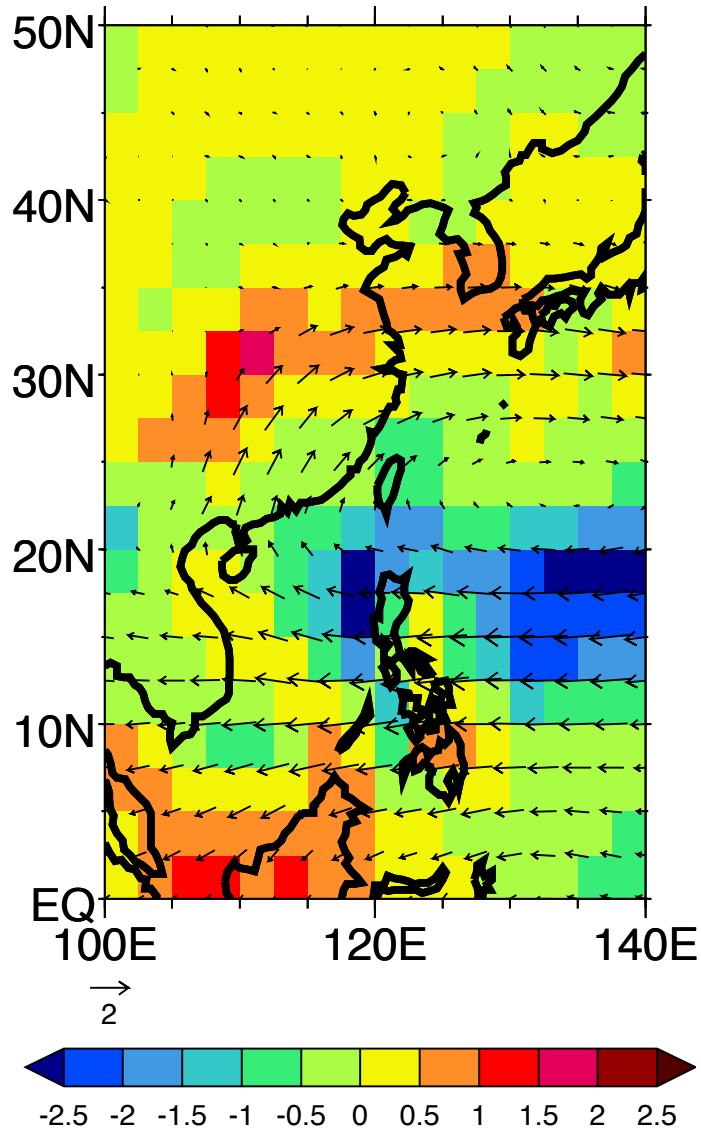
HadGEM2-ES



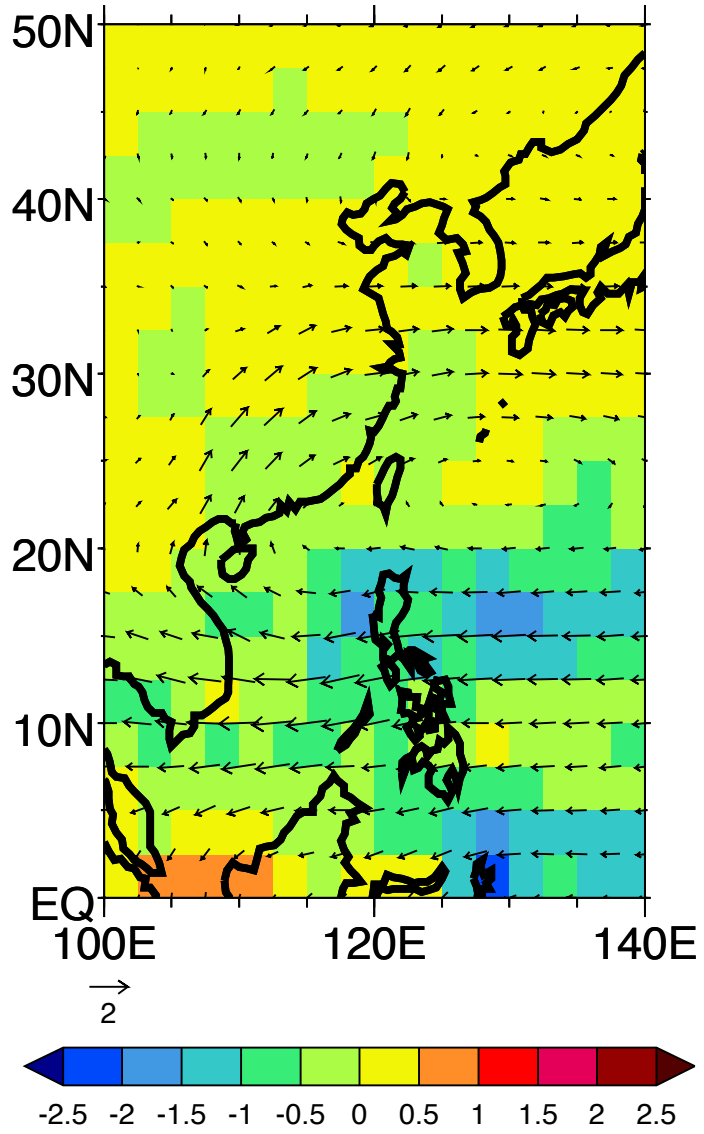
ukmo-hadcm3



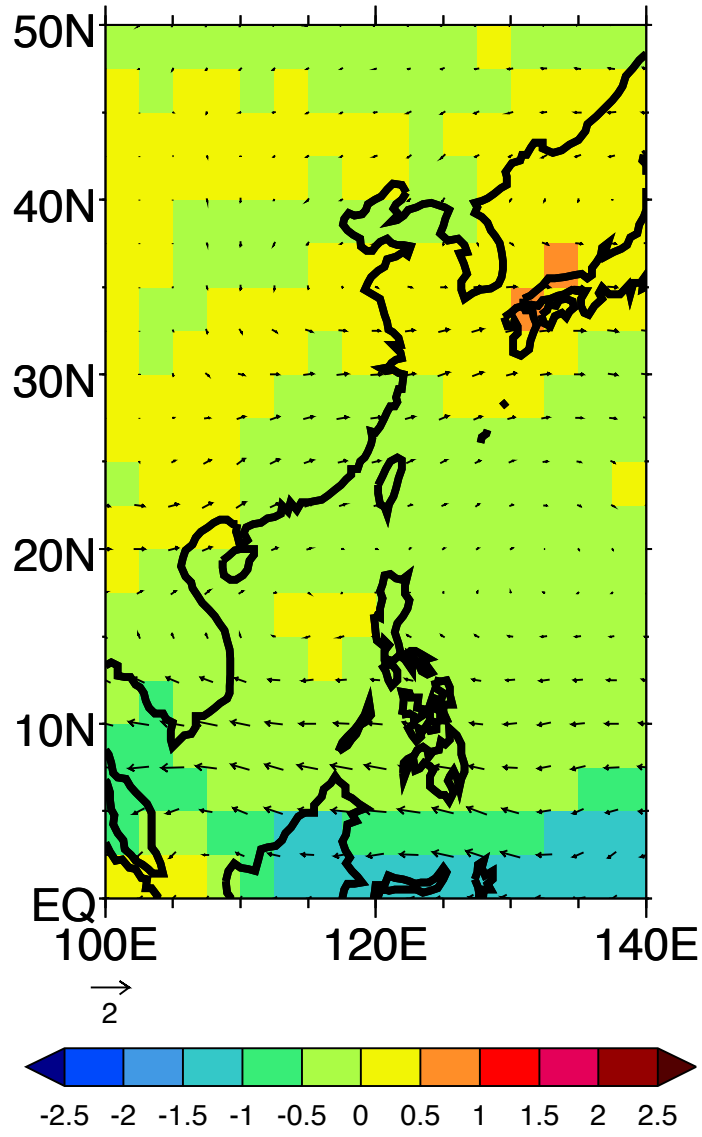
ukmo-hadgem1



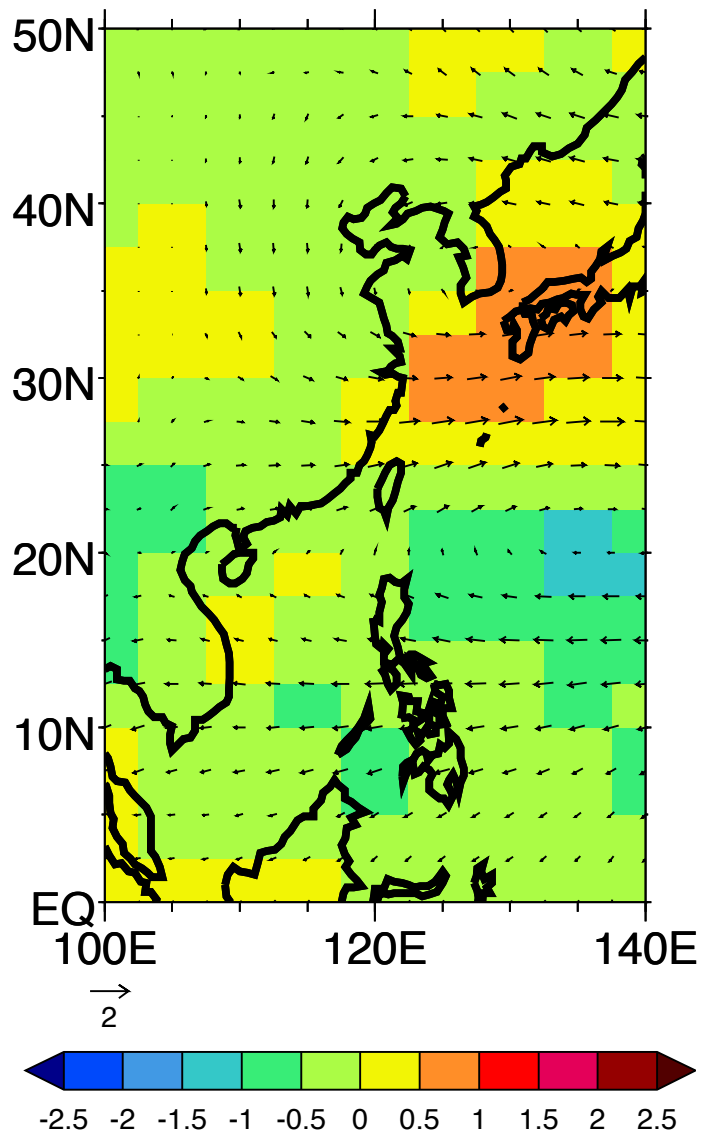
ingv-sxg



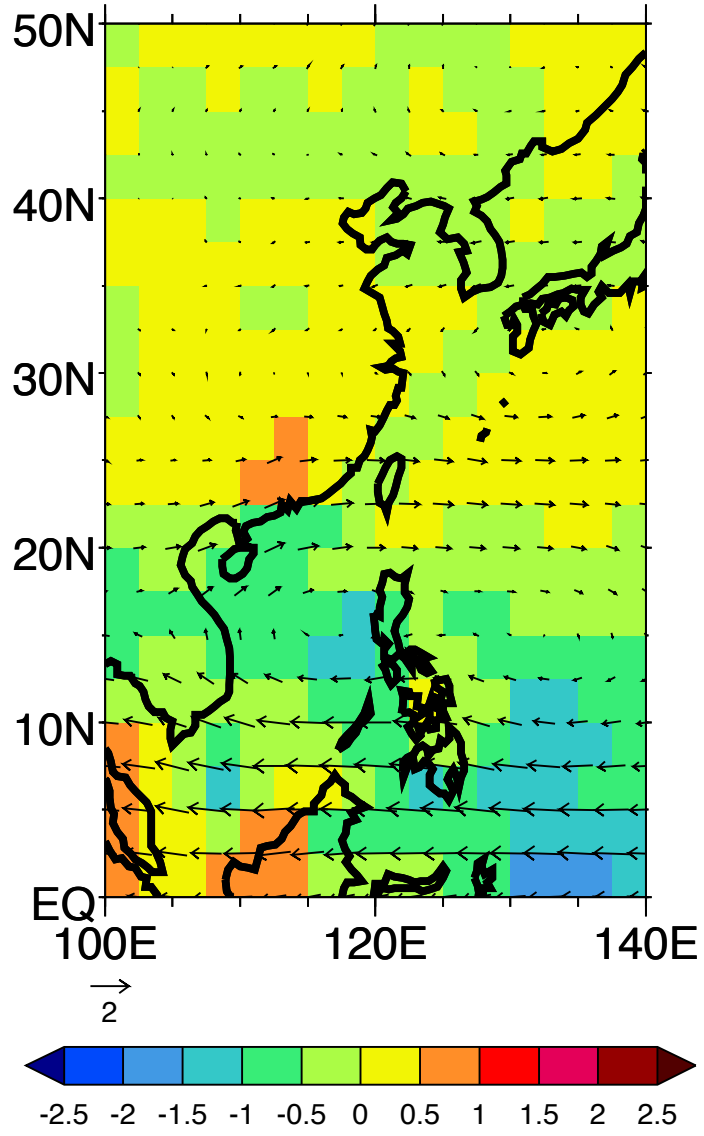
INM-CM4



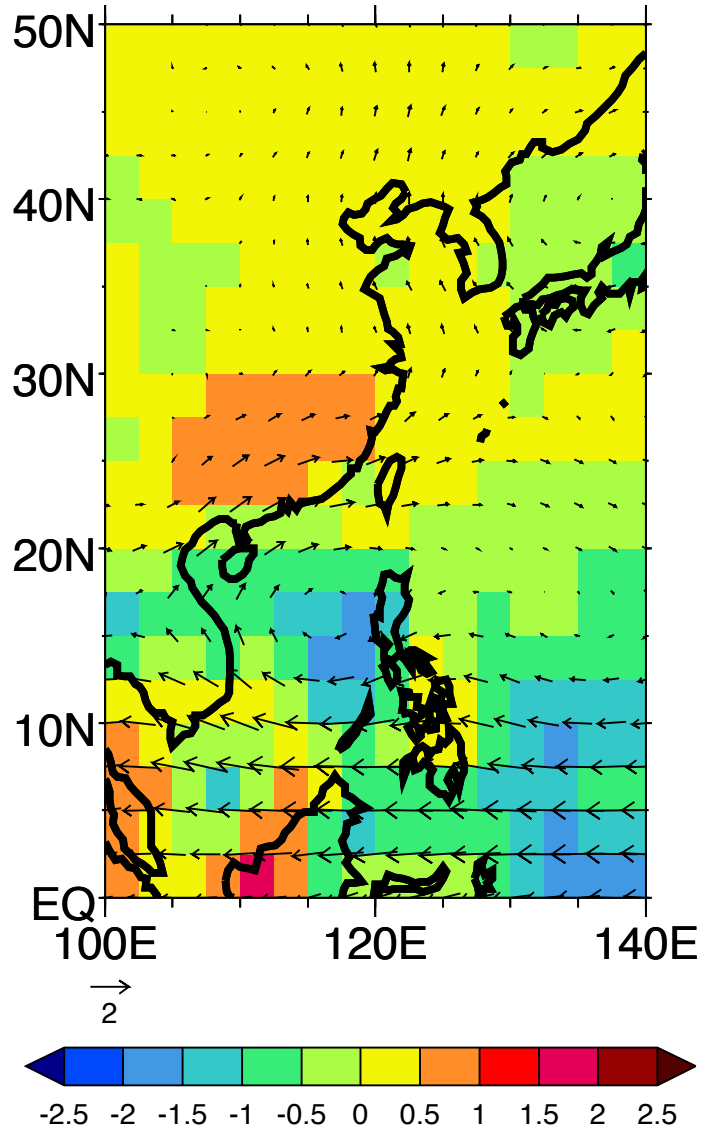
inm-cm3.0



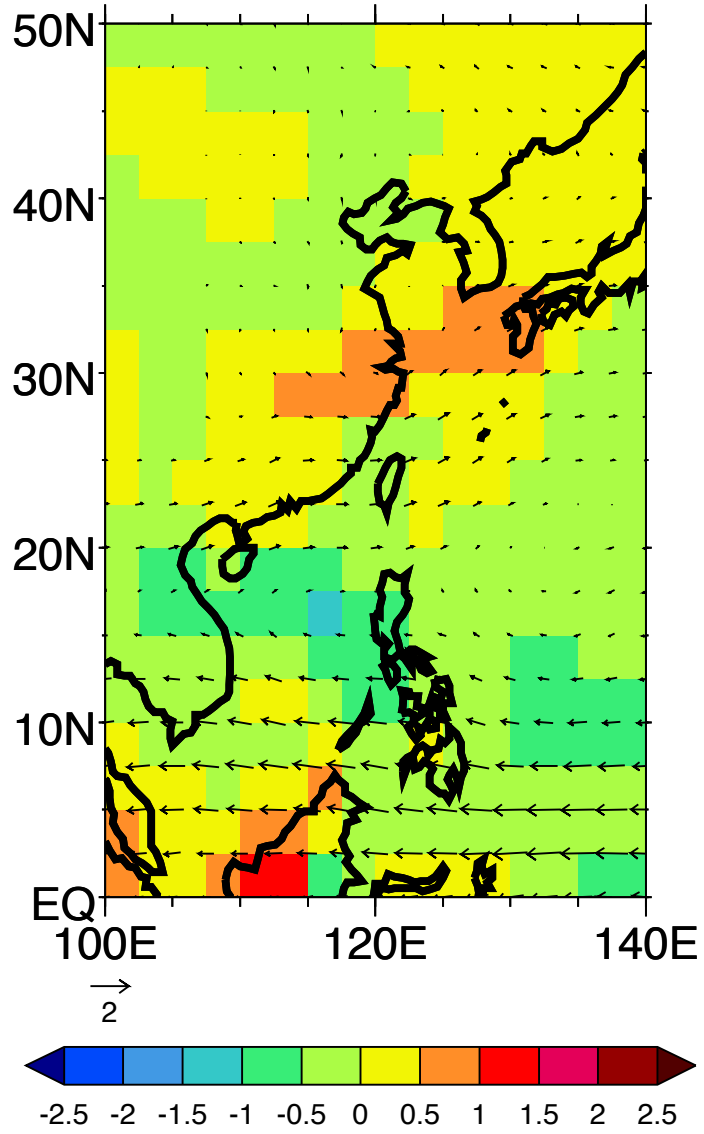
IPSL-CM5A-LR



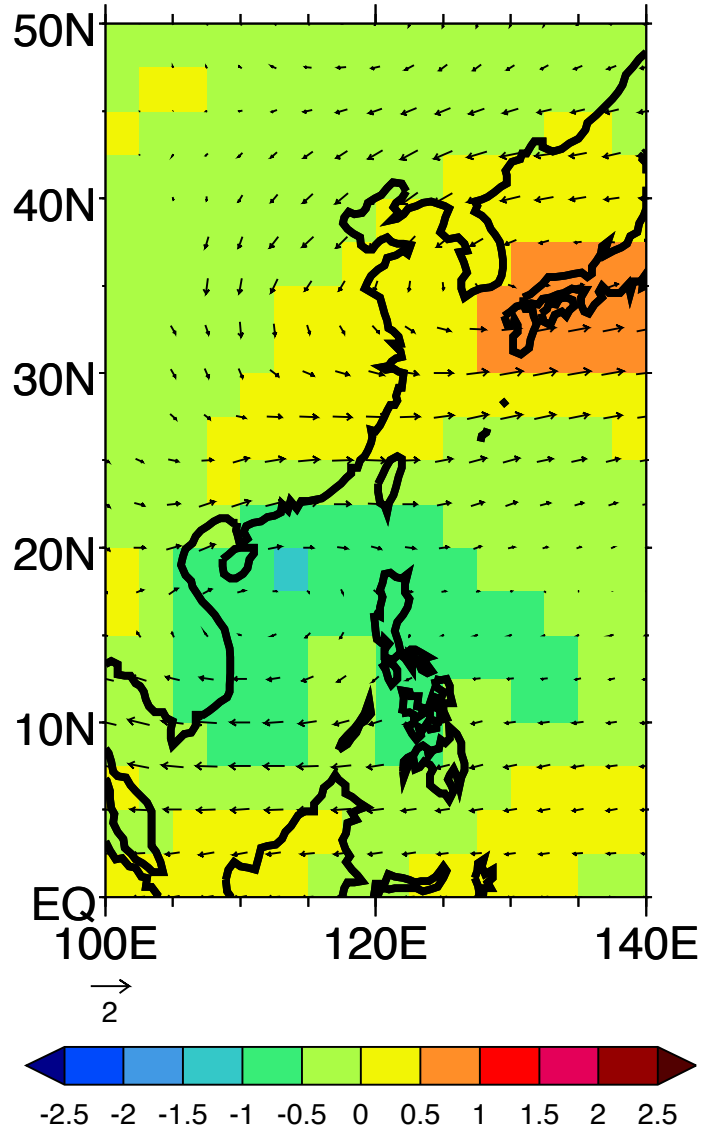
IPSL-CM5A-MR



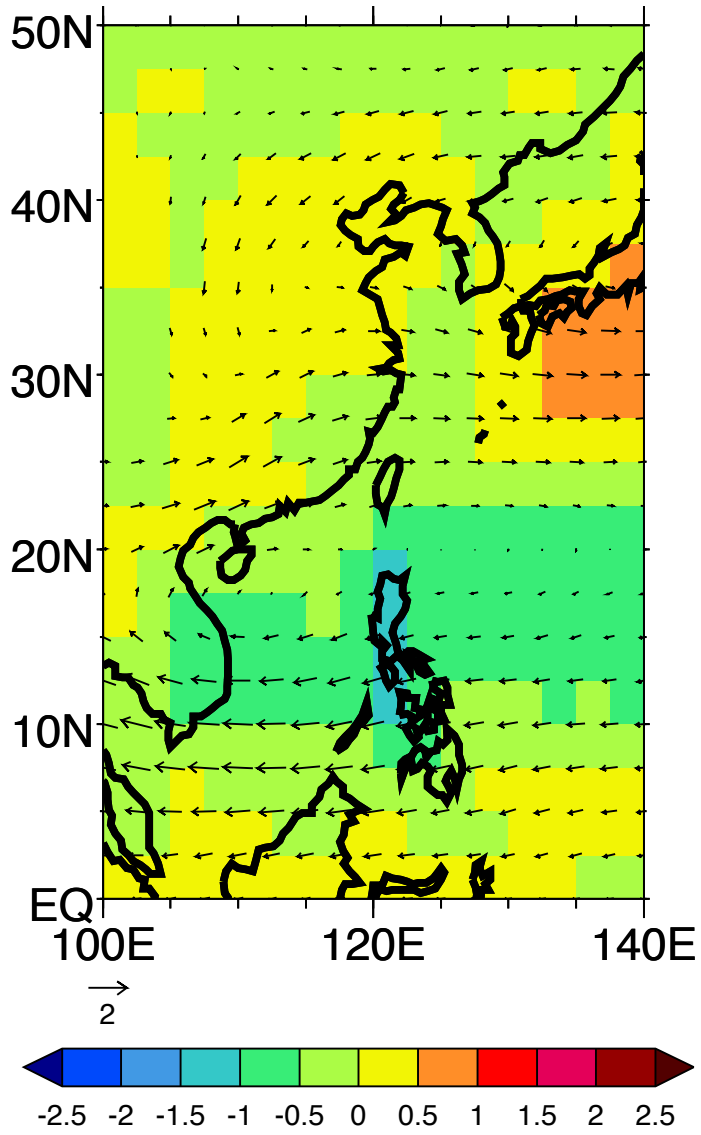
ipsl-cm4



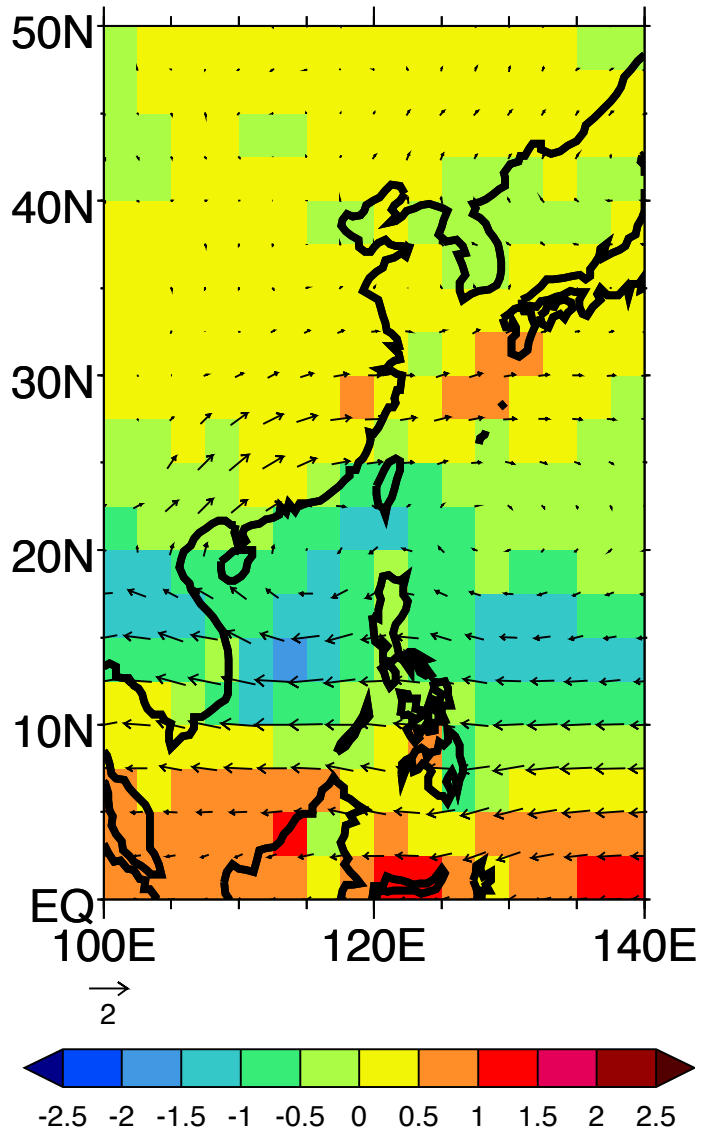
MIROC-ESM



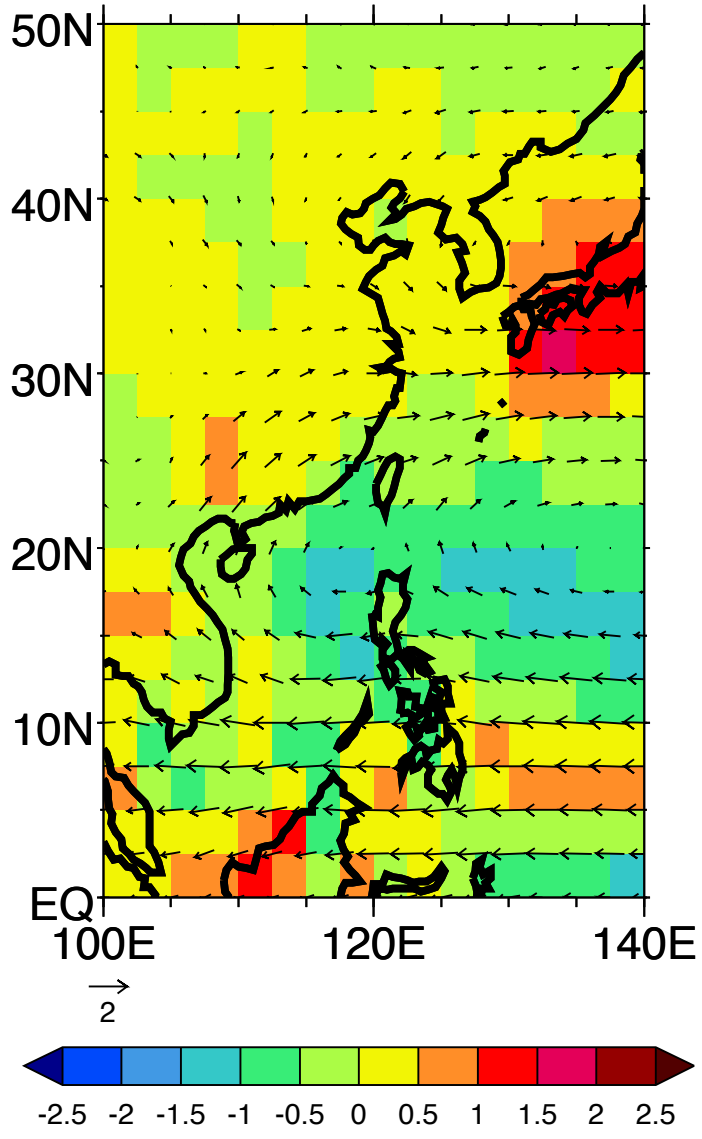
MIROC-ESM-CHEM



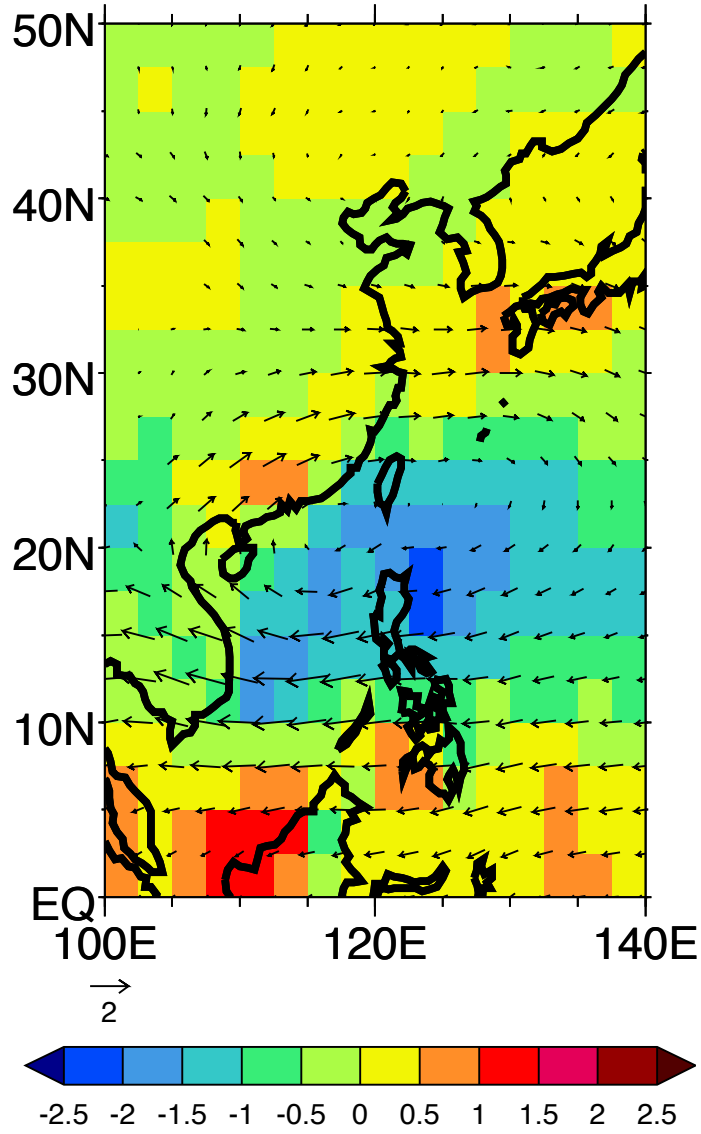
MIROC4h



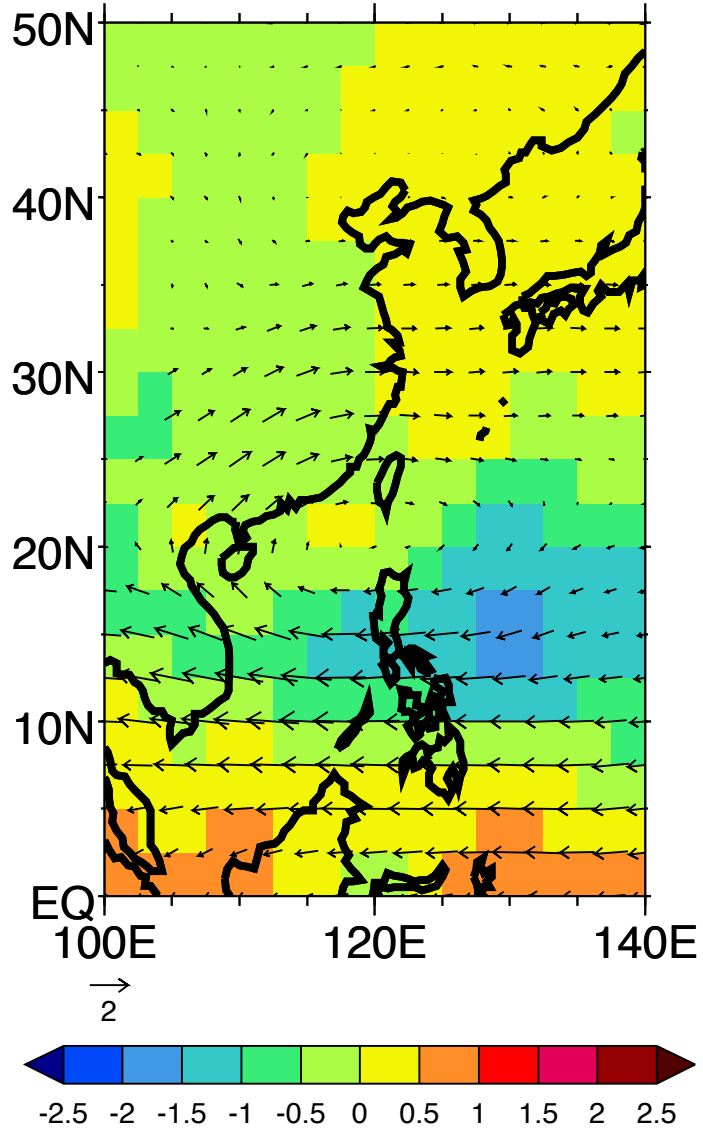
MIROC5



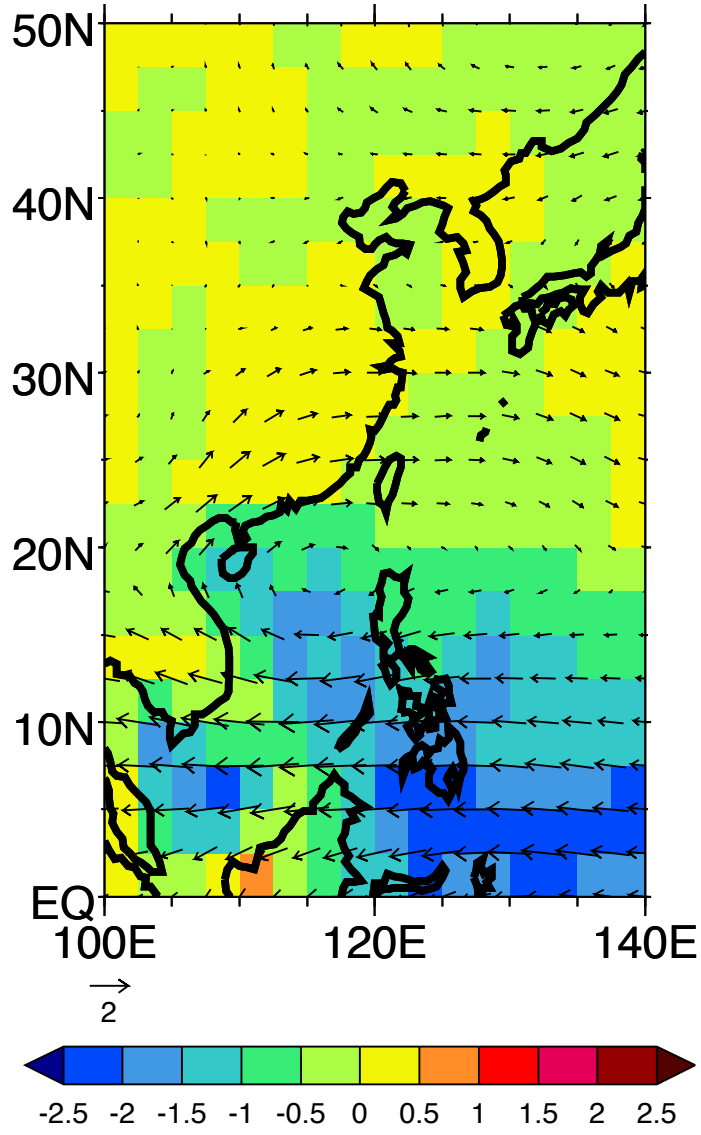
miroc3.2 (hires)



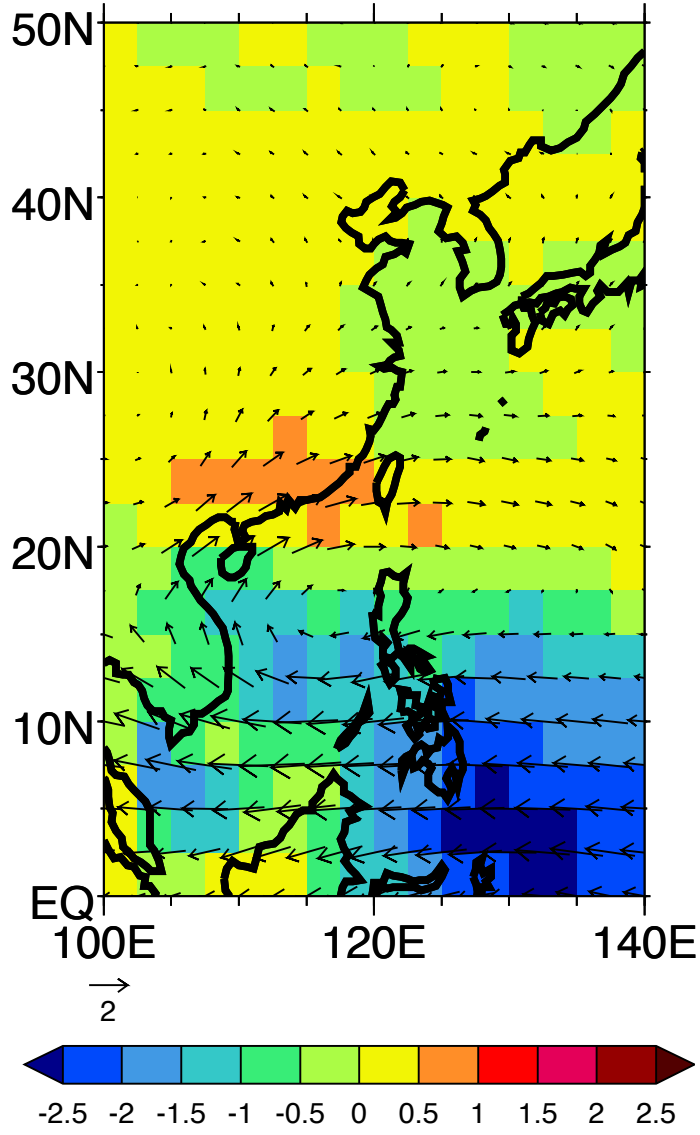
miroc3.2 (medres)



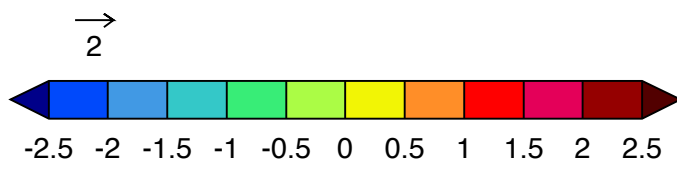
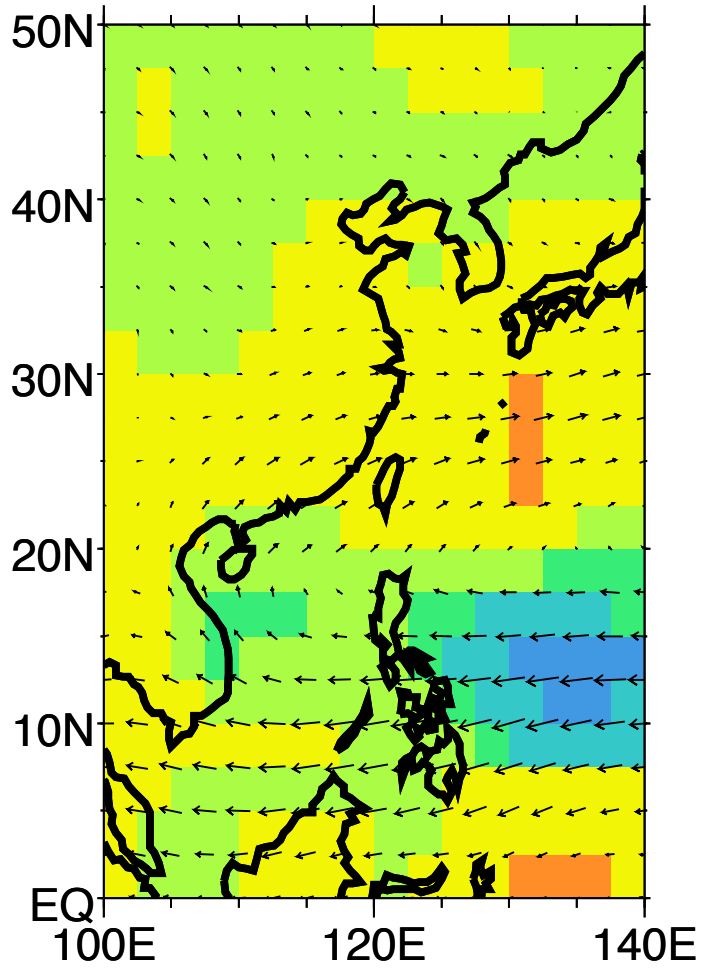
MPI-ESM-LR



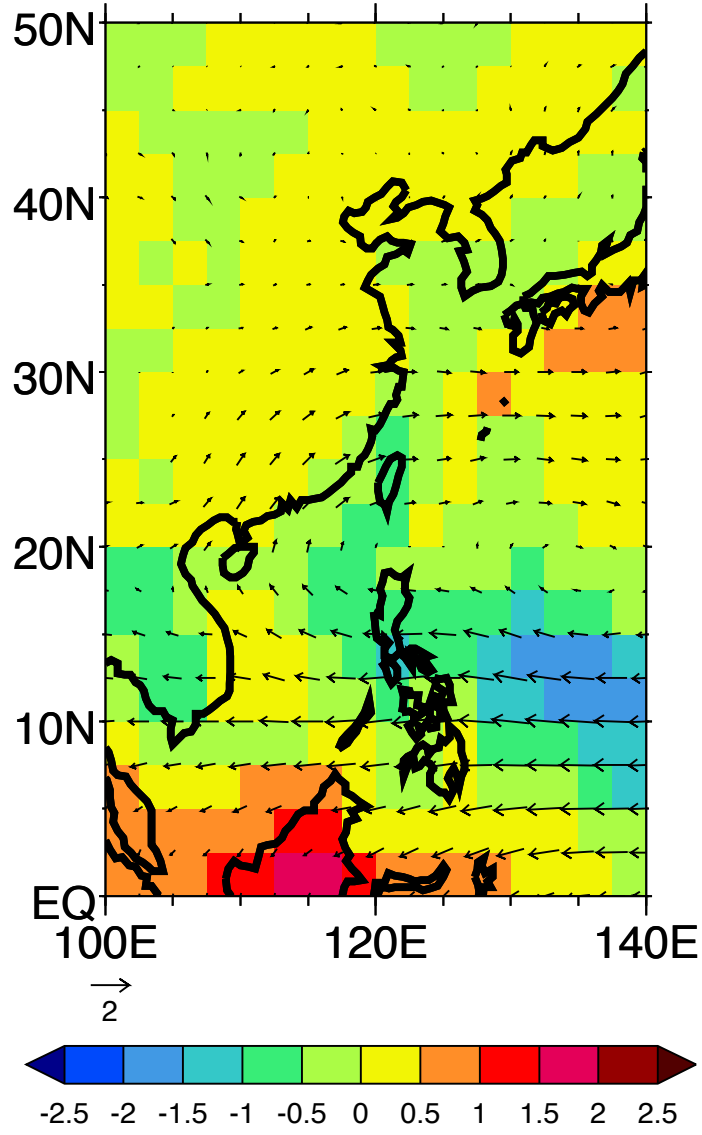
echam5/mpi-om



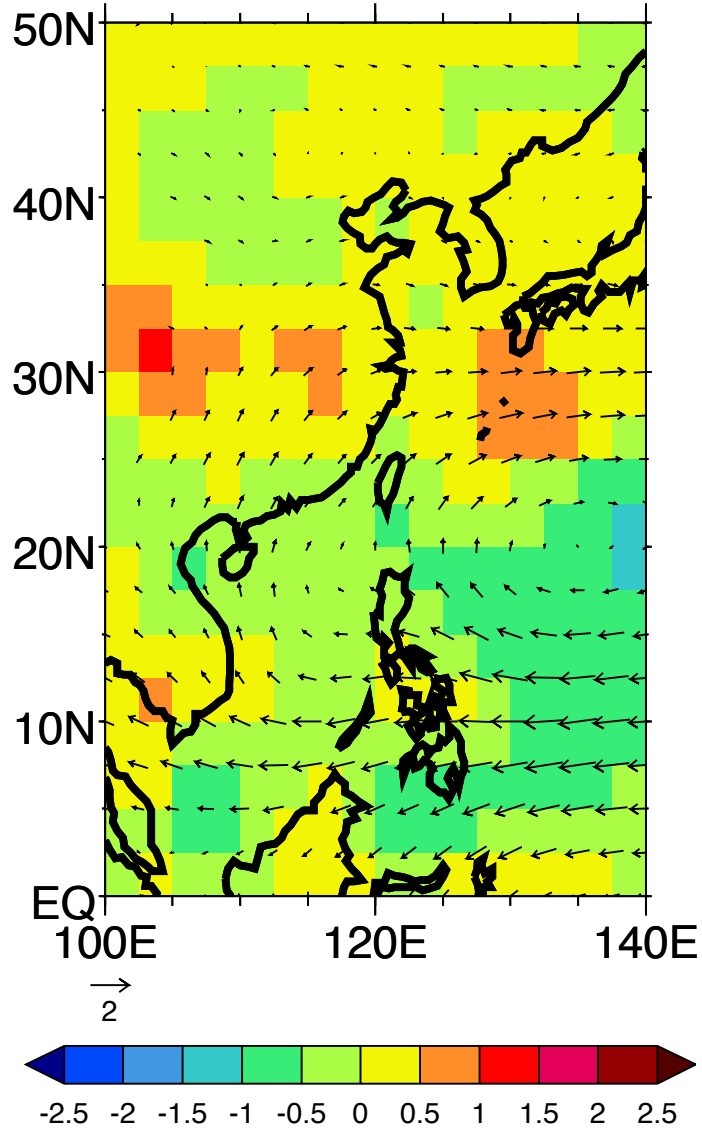
echo-g



MRI-CGCM3



mri-cgcm2.3.2



NorESM1-M

